

To appear in *Astrophys. J.* 535 (2000)

THE CORRELATION FUNCTION IN REDSHIFT SPACE: GENERAL FORMULA WITH WIDE-ANGLE EFFECTS AND COSMOLOGICAL DISTORTIONS

Takahiko Matsubara¹

Department of Physics and Astronomy, The Johns Hopkins University, 3400 N.Charles
Street, Baltimore, MD 21218

ABSTRACT

A general formula for the correlation function in redshift space is derived in linear theory. The formula simultaneously includes wide-angle effects and cosmological distortions. The formula is applicable to any pair with arbitrary angle θ between lines of sight, and arbitrary redshifts, z_1, z_2 , which are not necessarily small. The effects of the spatial curvature both on geometry and on fluctuation spectrum are properly taken into account, and thus our formula holds in a Friedman-Lemaître universe with arbitrary cosmological parameters Ω_0 and λ_0 . We illustrate the pattern of the resulting correlation function with several models, and also show that validity region of the conventional distant observer approximation is $\theta \leq 10^\circ$.

Subject headings: cosmology: theory — galaxies: distances and redshifts — quasars: general — large-scale structure of universe — methods: statistical

¹Department of Physics, The University of Tokyo, Hongo 7-3-1, Tokyo 113-0033, Japan; *and* Research Center for the Early Universe, Faculty of Science, The University of Tokyo, Tokyo 113-0033, Japan.

1. INTRODUCTION

Ever since the pioneering work of Totsuji & Kihara (1969) and Peebles (1974), the two-point correlation function of galaxies has been one of the most fundamental tools in analyzing the large-scale structure of the universe. Recently, prominent advances in galaxy redshift surveys have been taking place (for review, see Strauss 1999), and upcoming large-scale galaxy and QSO surveys, notably the Two-Degree Field Survey (2dF; Colless 1998; Folkes 1999), and the Sloan Digital Sky Survey (SDSS; Gunn & Weinberg 1995; Margon 1998), will provide three-dimensional, large-scale redshift maps of galaxies and QSO's. The two-point correlation function will play one of the central role in the analysis of such large-scale redshift maps.

In redshift surveys, the distances to objects are measured by recession velocities, and thus the distribution of objects in redshift space is not identical to that in real space. The clustering pattern is distorted by peculiar velocity fields (Kaiser 1987), and, for high redshift objects, also by cosmological warp of real space on a light-cone (Alcock & Paczyński 1979). Such effects are called as *redshift distortions*. These effects on the linear power spectrum and on the linear two-point correlation function have been investigated by many authors (for review, see Hamilton 1998)

Most of the work is for redshift distortions in a nearby universe and assumes $z \ll 1$. Kaiser (1987), in his seminal paper, derived the linear redshift distortions of the power spectrum for a nearby universe, employing the distant-observer approximation, which assumes the scales of fluctuations of interest are much smaller than the distances to the objects. Generally, the redshift distortions by peculiar velocities are along the line of sight. This radial nature of distortion introduces a statistical inhomogeneity into the redshift space. In the distant-observer approximation, such inhomogeneity is neglected and the statistical homogeneity is recovered, while the anisotropy is introduced, instead. The Fourier spectrum has maximal advantage when the statistical homogeneity does exist, thus, for this reason, Kaiser's formula has a very simple form. Hamilton (1992) transformed Kaiser's formula of the power spectrum to the formula of the two-point correlation function, using the Legendre expansion (see also Lilje & Efstathiou 1989; McGill 1990).

Despite the simple form of the formula, the distant-observer approximation is not desirable in the sense that we cannot utilize the whole information of the survey within this approximation. The wide-angle effect, which is the contribution of an angle θ between lines of sight of two objects to the correlation function, affects the analysis of the redshift maps when we intend to use the whole data of the survey. Therefore, the analysis of wide-angle effect on the correlation function in linear theory (Hamilton & Culhane 1996; Zaroubi & Hoffmann 1996; Szalay, Matsubara & Landy 1998; Bharadwaj 1999), as well as

the spherical harmonic analysis (Fisher, Scharf & Lahav 1994; Heavens & Taylor 1995), are of great importance.

All the above studies are for a nearby universe, and assume $z \ll 1$. This condition is not appropriate for modern galaxy redshift surveys ($z \sim 0.2$) or QSO redshift surveys ($z \sim 2$). The evolution of clustering and the nonlinearity in the redshift-distance relation introduce *the cosmological redshift distortion* on the correlation function. Ballinger, Peacock & Heavens (1996) and Matsubara & Suto (1996) explored this effect in power spectrum and correlation function, respectively, both employing the distant-observer approximation (see also Nakamura, Matsubara & Suto 1997; de Laix & Starkman 1997; Popowski et al. 1998; Nishioka & Yamamoto 1999; Nair 1999). The more the depth of the redshift surveys is increasing, the more the cosmological redshift distortion becomes important.

So far the previous formulas for two-point correlation function in redshift space are restricted either to nearby universe, or to distant-observer approximation. The purpose of the present paper is to derive the unified formula for the linear redshift distortions of the correlation function, fully taking into account the wide-angle effects and cosmological distortions, simultaneously. In this way, we do not have to think about which formula we should use depending on the value of z and θ . In addition, the effects of the spatial curvature are also included in our formulation and our formula applies to Friedman-Lemaître universe with arbitrary cosmological parameters Ω_0 and λ_0 . Our formula turns out to correctly reproduce the known results if we take appropriate limits of the formula.

In §2, the redshift-space distortions of density fluctuations toward radial directions are derived on a light-cone, which include the evolutionary effects. In §3, the formula for correlation function in redshift space is derived separately for open, flat, and closed models. Demonstrations of redshift distortions in several cases and the validity region of the conventional distant observer approximation are given in §4. The conclusions are summarized in §5.

2. LINEAR REDSHIFT-SPACE DISTORTIONS ON A LIGHT-CONE

2.1. Radial Distortion of Linear Density Field on a Light-cone

Throughout the present paper, we assume the Friedman-Lemaître-Robertson-Walker (FLRW) metric as the background space-time of the universe. According to the sign of the

spatial curvature K , the metric is given by

$$ds^2 = -c^2 dt^2 + \begin{cases} \frac{a^2(t)}{-K} [d\chi^2 + \sinh^2 \chi (d\theta^2 + \sin^2 \theta d\phi^2)], & (K < 0) \\ a^2(t) [d\chi^2 + \chi^2 (d\theta^2 + \sin^2 \theta d\phi^2)], & (K = 0) \\ \frac{a^2(t)}{K} [d\chi^2 + \sin^2 \chi (d\theta^2 + \sin^2 \theta d\phi^2)], & (K > 0) \end{cases} \quad (2.1)$$

where θ and ϕ are usual angular coordinates, and χ is a radial comoving coordinate. In the following, we choose a unit system, $c = 1$, and $H_0 = 1$, where $H_0 = 100 h \text{ km/s/Mpc}$ is the Hubble's constant, so that comoving distances are measured in units of $cH_0^{-1} = 2997.9 h^{-1} \text{ Mpc}$. In this unit system, the spatial curvature K is then given by

$$K = \Omega_0 + \lambda_0 - 1, \quad (2.2)$$

where the scale factor at present is normalized as $a_0 = 1$. From the FLRW metric, we define the three dimensional metric γ_{ij} as

$$ds^2 = -dt^2 + a^2 \gamma_{ij} dx^i dx^j. \quad (2.3)$$

That is, the tensor γ_{ij} is the metric for a three-space of uniform spatial curvature K . In the following, vectors with Latin indices represent the three-vector in the three-space specified by the metric γ_{ij} .

The comoving distance x at redshift z is given by

$$x(z) = \int_0^z \frac{dz'}{H(z')}, \quad (2.4)$$

where $H(z)$ is the Hubble parameter at (comoving) redshift z :

$$H(z) = \sqrt{(1+z)^3 \Omega_0 + (1+z)^2 (1 - \Omega_0 - \lambda_0) + \lambda_0}. \quad (2.5)$$

The radial comoving coordinate χ and the comoving distance x are related by

$$\chi = \begin{cases} |K|^{1/2} x(z), & (K \neq 0) \\ x(z). & (K = 0) \end{cases} \quad (2.6)$$

Provided that a cosmological model is fixed, the comoving distance χ , and the redshift z are related through equation (2.6) on the observable past light-cone, and we interchangeably use these variables in the following. Therefore, we use the redshift z as an alternative spatial coordinate. On a light cone surface, it is also considered as an alternative of the time variable, t .

In this paper, the light ray is assumed to be transmitted on an unperturbed metric for simplicity. This point is discussed later. Then, in redshift space, the angular coordinates (θ, ϕ) are common to those in real space. Only the radial distances are distorted in redshift space. Let us consider an object located at comoving coordinates (t, x^i) which has the 4-velocity u^μ , normalized as $u^\mu u_\mu = -1$ as usual. In terms of the three-dimensional peculiar velocity v^i , this 4-velocity is given by

$$u^\mu = \frac{(1, v^i)}{\sqrt{1 - a^2 v^i v_i}}. \quad (2.7)$$

The wave 4-vector, k^μ , satisfying the null geodesic equations, $k^\mu k_\mu = 0$ and $k^\mu_{;\nu} k^\nu = 0$, is given by

$$k^\mu \propto (a^{-1}, -a^{-2} n^i), \quad k_\mu \propto (-a^{-1}, -n_i), \quad (2.8)$$

where n^i is a three dimensional normal vector, which represents the line of sight, and $n_i = \gamma_{ij} n^j$. The frequencies of the light at the source and at the observer are given by $\nu_1 = (k_\mu u^\mu)|_t$, and $\nu_0 = (k_\mu u^\mu)|_{t_0}$, respectively. Assuming the peculiar velocities are non-relativistic, the redshift z_{obs} the observer actually observes is given by

$$1 + z_{\text{obs}} = \frac{\nu_1}{\nu_0} = (1 + z)(1 + W - W_0) \quad (2.9)$$

where $W = a n_i v^i$ and $W_0 = n_i v_0^i$ are the line-of-sight components of peculiar velocities of the source and of the observer. The peculiar velocity W is evaluated on a light cone, and W_0 can be estimated from the value of the dipole anisotropy of cosmic microwave background radiation.

For convenience, we define the redshift-space physical comoving distance as $s(z) = x(z_{\text{obs}})$ where z_{obs} is given by the equation (2.9), and the function $x(z)$ is formally the same as equation (2.4) by definition. Explicitly, $s(z)$ is defined by

$$s(z) = \int_0^{z+(1+z)(W-W_0)} \frac{dz'}{H(z')}. \quad (2.10)$$

In other words, the redshift-space physical comoving distance s defined by equation (2.10) is the apparent physical comoving distance of an object in redshift space, which is originally at redshift z in real space, and is shifted by its own peculiar velocity. In a limit $z_{\text{obs}} \rightarrow 0$, equation (2.10) reduces to the usual relation for nearby universe (Kaiser 1987), $s = z_{\text{obs}}/H_0 = x + (W - W_0)/H_0$. From the redshift-space physical comoving distance s , we also define the redshift-space analog of comoving coordinate, χ_s as $\chi_s(z) = \chi(z_{\text{obs}})$, or equivalently,

$$\chi_s = \begin{cases} |K|^{1/2} s(z), & (K \neq 0) \\ s(z). & (K = 0) \end{cases} \quad (2.11)$$

The difference between the number density of observed objects in real space, $n^{(r)}(\chi, \theta, \phi, t)$ and that in redshift space, $n^{(s)}(\chi_s, \theta, \phi)$, are related by the number conservation:

$$\begin{aligned} n^{(s)}(\chi_s, \theta, \phi) \sinh^2 \chi_s d\chi_s d\Omega &= n^{(r)}(\chi, \theta, \phi) \sinh^2 \chi d\chi d\Omega, & (K < 0) \\ n^{(s)}(\chi_s, \theta, \phi) \chi_s^2 d\chi_s d\Omega &= n^{(r)}(\chi, \theta, \phi) \chi^2 d\chi d\Omega, & (K = 0) \\ n^{(s)}(\chi_s, \theta, \phi) \sin^2 \chi_s d\chi_s d\Omega &= n^{(r)}(\chi, \theta, \phi) \sin^2 \chi d\chi d\Omega, & (K > 0) \end{aligned} \quad (2.12)$$

where $d\Omega = \sin \theta d\theta d\phi$, and $n^{(r)}$ is evaluated on a light cone. Therefore,

$$n^{(s)}(\chi_s, \theta, \phi) = n^{(r)}(\chi, \theta, \phi) \times \begin{cases} \left(\frac{\sinh^2 \chi_s}{\sinh^2 \chi} \frac{\partial \chi_s}{\partial \chi} \right)^{-1}, & (K < 0) \\ \left(\frac{\chi_s^2}{\chi^2} \frac{\partial \chi_s}{\partial \chi} \right)^{-1}, & (K = 0) \\ \left(\frac{\sin^2 \chi_s}{\sin^2 \chi} \frac{\partial \chi_s}{\partial \chi} \right)^{-1}. & (K > 0) \end{cases} \quad (2.13)$$

The number density in real space is given by the underlying number density of objects ρ multiplied by the selection function Φ :

$$n^{(r)}(\chi, \theta, \phi) = \Phi(\chi, \theta, \phi) \rho(\chi, \theta, \phi) \quad (2.14)$$

where we allow the direction dependence of the selection function.

We assume the linear theory of density fluctuation throughout this paper and we only consider the first order in perturbation with respect to the variables, W , W_0 , and $\delta = \rho/\bar{\rho} - 1$. Then the relation between χ_s and χ for a fixed z , equation (2.10) becomes

$$\chi_s = \chi + \frac{1+z}{H(z)}(U - U_0), \quad (2.15)$$

where $U = |K|^{1/2}W$, $U_0 = |K|^{1/2}W_0$, for non-flat universe and $U = W$, $U_0 = W_0$, for flat universe. With this expansion, the density contrast $\delta^{(s)}$ up to the first order is given by

$$\begin{aligned} \delta^{(s)}(\chi, \theta, \phi) &= \frac{n^{(s)}(\chi_s, \theta, \phi)}{\bar{\rho}\Phi(\chi_s, \theta, \phi)} - 1 \\ &= \delta(\chi, \theta, \phi) - \frac{\partial}{\partial \chi} \left(\frac{U}{aH} \right) - \frac{A(\chi)}{aH} U + \left(\frac{A(\chi)}{aH} - \tilde{q}_{\text{dec}} \right) U_0, \end{aligned} \quad (2.16)$$

where

$$A(\chi) = \begin{cases} \frac{\cosh \chi}{\sinh \chi} \left(2 + \frac{\partial \ln \Phi}{\partial \ln \sinh \chi} \right), & (K < 0) \\ \frac{1}{\chi} \left(2 + \frac{\partial \ln \Phi}{\partial \ln \chi} \right), & (K = 0) \\ \frac{\cos \chi}{\sin \chi} \left(2 + \frac{\partial \ln \Phi}{\partial \ln \sin \chi} \right), & (K > 0) \end{cases} \quad (2.17)$$

and $\tilde{q}_{\text{dec}}(z) = -d(a^{-1}H^{-1})/d\chi$, $\Omega = 8\pi G\rho/(3H^2)$ and $\lambda = \Lambda/(3H^2)$ are the normalized time-dependent deceleration parameter, the time-dependent density parameter and the dimensionless cosmological term, respectively. The parameter \tilde{q}_{dec} is equal to the usual time-dependent deceleration parameter $\Omega/2 - \lambda$ for flat universe, and $|K|^{-1/2}$ times the usual deceleration parameter for non-flat universe. The light-cone effect of density contrast in redshift space is represented by this equation (2.16). It is obvious that this equation is a generalization of corresponding formula derived by Kaiser (1987) for $z \rightarrow 0$.

In the above equations, the light ray is assumed to be transmitted on an unperturbed metric. In reality, the frequency of the light is altered by the Sachs-Wolfe effect (Sachs & Wolfe 1967), and the path is bent by the gravitational lensing effect. The Sachs-Wolfe effect is the contribution of the potential fluctuations to the estimate of the redshift. The potential fluctuations are negligible except on scales comparable to the Hubble distance, and in reality, observational determination of the fluctuations on Hubble scales is not easy. Therefore, the Sachs-Wolfe effect on the correlation function of density field is not supposed to be important in practice.

The gravitational lensing changes the position on the sky of the observable objects. The weak lensing (Kaiser 1992, 1998; Bernardeau, Waerbeke, & Mellier 1997) is relevant in our linear analysis. The estimate of the number density is turn out to be affected by the local convergence of the gravitational lensing. The local convergence is given by the integration of the density fluctuations along the line of sight (Bernardeau et al. 1997), and it is efficient for $z \gtrsim 1$. Therefore, it is possible that the gravitational lensing affects the correlation function for $z \gtrsim 1$. In which case, we should add a correction term to the equation (2.16). The quantitative estimate of this effect is beyond the scope of this paper, and will be investigated in a future paper.

2.2. Redshift-space Distortion Operator

The equations of motion relate the density contrast δ and the velocity field U . Since we intend to include the curvature effect, the Newtonian equations of motion are not appropriate. Instead, we employ the perturbed Einstein equation,

$$\delta G^\mu{}_\nu = 8\pi G\delta T^\mu{}_\nu, \quad (2.18)$$

on a background FLRW metric. In order to avoid the inclusion of spurious gauge modes in the solution, Bardeen (1980) introduced the gauge-invariant formalism for the above perturbed equation (see also Kodama & Sasaki 1984; Abbott & Schaefer 1986; Hwang & Vishniac 1990). In Appendix A, we review the gauge-invariant formalism for the

pressureless fluid, and derive complete equations to determine the evolution of the density contrast and the velocity field. They are given by equations (A22)–(A24):

$$\dot{\delta} + (\Delta + 3K)\psi = 0, \quad (2.19)$$

$$\dot{\psi} + 2H\psi + \Phi = 0, \quad (2.20)$$

$$(\Delta + 3K)\Phi = \frac{3}{2}H^2\Omega\delta, \quad (2.21)$$

where a dot denotes the differentiation with respect to the proper time, d/dt , and $\Delta = \nabla^i \nabla_i$ is the Laplacian on the 3-metric, γ_{ij} of the FLRW metric, which is explicitly given in Appendix B, equation (B1). As shown in Appendix A, the transverse part of the velocity field decays with time as a^{-2} and can be neglected, thus the velocity is characterized by the velocity potential ψ so that the velocity is given by $v^i = \nabla^i \psi$. The variables δ , ψ , and Φ in the above equations are actually gauge-invariant linear combinations defined in Appendix A, and are guaranteed not to have spurious gauge mode in the solution. These variables correspond to density contrast, velocity potential, and gravitational potential inside the particle horizon. In general, δ and v correspond to the density contrast and velocity in velocity-orthogonal isotropic gauge, $V = B$, $H_T = 0$, in the notation of Appendix A. It is obvious that equations (2.19)–(2.21) correspond to the continuity, Euler, and Poisson equations in Newtonian linear theory. The only difference is the appearance of the curvature term in the Laplacian. The curvature term would not be important in practice because the correlation function on curvature scales is too small to be practically detectable. However, we retain the curvature term for theoretical consistency in the following.

Eliminating the variables ψ and Φ from the equations, we obtain the evolution equation for the Bardeen’s gauge-invariant density contrast δ , given by

$$\ddot{\delta} + 2H\dot{\delta} - \frac{3}{2}H^2\Omega\delta = 0. \quad (2.22)$$

This equation is equivalent to that in Newtonian theory for the density contrast, and the solution of this equation is well-known (Peebles 1980). The time dependence of the growing solution is given by

$$D(t) \propto a\Omega \int_0^1 \frac{dx}{(\Omega/x + \lambda x^2 + 1 - \Omega - \lambda)^{3/2}}. \quad (2.23)$$

In the following, we normalize this growing factor as $D(t_0) = 1$, where t_0 is the present time. Thus, the growing solution of the equation (2.22) is given by

$$\delta(\chi, \theta, \phi, t) = D(t)\delta_0(\chi, \theta, \phi), \quad (2.24)$$

where $\delta_0 \equiv \delta(t = t_0)$ is the mass density contrast at the present time.

Equation (2.19) gives the solution of the velocity potential as

$$\psi = -HDf(\Delta + 3K)^{-1}\delta_0, \quad (2.25)$$

where $f = (a/D)dD/da = \dot{D}/(HD)$ and $H = \dot{a}/a$ is the Hubble parameter at time t . The inverse operator $(\Delta + 3K)^{-1}$ is evaluated by spectral decomposition in the next section. It turns out that the function f depends only on Ω and λ , and is approximately given by (Lahav et al. 1991)

$$f = \Omega^{0.6} + \frac{\lambda}{70} \left(1 + \frac{\Omega}{2}\right). \quad (2.26)$$

From equation (2.25),

$$W = an^i \nabla_i \psi = aHDf \frac{\partial}{\partial x} (\Delta + 3K)^{-1} \delta_0. \quad (2.27)$$

Since $\partial/\partial x = |K|^{1/2} \partial/\partial \chi$ for non-flat universe and $\partial/\partial x = \partial/\partial \chi$ for flat universe, the above equation is equivalent to

$$U(\chi, \theta, \phi) = aHDf \times \begin{cases} |K| \partial_\chi (\Delta + 3K)^{-1} \delta_0(\chi, \theta, \phi), & (K \neq 0) \\ \partial_\chi \Delta^{-1} \delta_0(\chi, \theta, \phi), & (K = 0) \end{cases} \quad (2.28)$$

where $\partial_\chi = \partial/\partial \chi$.

Equations (2.16) and (2.28) indicate the linear operator which transforms the density contrast at present in real space to that in redshift space on a light-cone. That is, we can define the redshift distortion operator:

$$\hat{R} = 1 + \beta \times \begin{cases} |K| (\partial_\chi + \alpha) \partial_\chi (\Delta + 3K)^{-1}, & (K \neq 0) \\ (\partial_\chi + \alpha) \partial_\chi \Delta^{-1}, & (K = 0) \end{cases} \quad (2.29)$$

where

$$\alpha(\chi) = \begin{cases} \frac{\cosh \chi}{\sinh \chi} \left(2 + \frac{\partial \ln(Df\Phi)}{\partial \ln \sinh \chi}\right), & (K < 0) \\ \frac{1}{\chi} \left(2 + \frac{\partial \ln(Df\Phi)}{\partial \ln \chi}\right), & (K = 0) \\ \frac{\cos \chi}{\sin \chi} \left(2 + \frac{\partial \ln(Df\Phi)}{\partial \ln \sin \chi}\right). & (K > 0) \end{cases} \quad (2.30)$$

The time-dependent redshift distortion parameter is defined by $\beta(z) = f(z)/b(z)$, where $b(z)$ is the time-dependent bias parameter. In the following, we present the result in the case that there is neither stochasticity nor scale-dependence in the biasing. It is straightforward

to include the scale-dependence and stochasticity, although the expression becomes more tedious. In linear regime, however, the stochasticity is shown to asymptotically vanish on large scales and biasing is scale-independent beyond the scale of galaxy formation, except some special cases (Matsubara 1999).

For the surveys of nearby universe, $z \ll 1$, the functions D and f do not vary as rapidly as the selection function, Φ , and the factor Df in the above equations can be omitted, as is done in the literatures. However, if the selection function varies as slowly as the factor Df , the latter factor cannot be neglected. With the redshift distortion operator, we can re-express the density contrast in redshift space as

$$\delta^{(s)}(x, \theta, \phi) = bD\hat{R}\delta_0(x, \theta, \phi) + \left(\frac{1+z}{H(z)}A(\chi) - q_{\text{dec}}(z) \right) U_0. \quad (2.31)$$

This expression depends on a peculiar motion of observer, U_0 , which somewhat complicate the analysis. Since we know the value U_0 by measuring the dipole anisotropy of the CMB radiation (Kogut et al. 1993; Lineweaver et al. 1996), we can subtract the term which depends on U_0 from the above expression. In the following we derive the correlation function in redshift space from the observer in the CMB frame and drop the U_0 term. In proper comparison of our result below and the observation, one should be sure that the correlation function is corrected by such kind of transformation to the CMB frame (Hamilton 1998).

The correlation function in redshift space of two points, $\mathbf{x}_1, \mathbf{x}_2$ is thus given by

$$\xi^{(s)}(\mathbf{x}_1, \mathbf{x}_2) = b_1 b_2 D_1 D_2 \hat{R}_1 \hat{R}_2 \xi(\chi). \quad (2.32)$$

where $b_1 = b(z_1)$, $b_2 = b(z_2)$, $D_1 = D(z_1)$, $D_2 = D(z_2)$, and z_1, z_2 are redshifts of the two points, and $\xi(\chi)$ is the mass correlation function in real space at present time. The redshift distortion operators \hat{R}_1 and \hat{R}_2 operate the density contrast at points \mathbf{x}_1 and \mathbf{x}_2 , respectively, and χ is a comoving separation of the two points. If we do not omit the local velocity term, U_0 , the square of the second term in equation (2.31) is added to the equation (2.32). In the following, we obtain an explicit expression for equation (2.32).

3. THE CORRELATION FUNCTION IN REDSHIFT SPACE IN FRIEDMAN-LEMAÎTRE UNIVERSES

In this section, we derive the explicit expression for the correlation function in redshift space. We separately consider an open universe, a flat universe and a closed universe in the following subsections.

3.1. An Open Universe

In an open universe ($K < 0$), the correlation function in real space is given by equation (B51):

$$\xi(\chi) = \int \frac{\nu^2 d\nu}{2\pi^2} X_0(\nu, \chi) S(\nu), \quad (3.1)$$

where

$$X_0 = \frac{\sin \nu \chi}{\nu \sinh \chi}, \quad (3.2)$$

and $S(\nu)$ is the power spectrum of the gauge-invariant density contrast (see Appendix B for detail)². In this subsection, we omit the superscript $(-)$ of X_l , which distinguish the difference of functional forms according to the sign of curvature in Appendix B. Equation (2.32) implies that we only need to calculate $\hat{R}_1 \hat{R}_2 X_0(\nu, \chi)$ to obtain the formula for correlation function in redshift space. Since the Laplacian is the invariant operator under transformation of the coordinate system, the inverse operation $(\Delta_1 + 3K)^{-1}$, $(\Delta_2 + 3K)^{-1}$ to X_0 is simply given by $(-q^2 + 3K)^{-1} X_0 = -|K|^{-1}(\nu^2 + 4)^{-1} X_0$, where q is defined by equation (B6), because X_0 is the fundamental eigenfunction of the Laplacian [Appendix B, equation (B2)].

The computationally nontrivial part of the redshift-space distortion operator is the spatial derivatives along the lines of sight, ∂_χ , which is not invariant operation, unlike the Laplacian. We illustrate in the rest of this subsection how the calculation can be accomplished. The comoving separation χ between \mathbf{x}_1 and \mathbf{x}_2 is related to the comoving distances χ_1 and χ_2 of these two points from the observer and the angle, θ between the lines of sight of these points with respect to the observer (Figure 1), through the standard relation:

$$\cosh \chi = \cosh \chi_1 \cosh \chi_2 - \sinh \chi_1 \sinh \chi_2 \cos \theta. \quad (3.3)$$

The derivatives of this equation yield

$$\frac{\partial \chi}{\partial \chi_1} = \frac{1}{\sinh \chi} (\sinh \chi_1 \cosh \chi_2 - \cosh \chi_1 \sinh \chi_2 \cos \theta) = \cos \gamma_1, \quad (3.4)$$

$$\frac{\partial \chi}{\partial \chi_2} = \frac{1}{\sinh \chi} (\cosh \chi_1 \sinh \chi_2 - \sinh \chi_1 \cosh \chi_2 \cos \theta) = \cos \gamma_2, \quad (3.5)$$

²Note that the power spectrum near the horizon scale depends on the gauge choice. The power spectrum $S(\nu)$ is defined by Bardeen's gauge-invariant density contrast, i.e., the density contrast in a gauge with velocity-orthogonal slicing, $V = B$.

where γ_1 is an angle between the geodesics of χ_1 and χ , and γ_2 is an angle between the geodesics of χ_2 and χ (Figure 1). The following equations are useful for our purpose:

$$\frac{\partial}{\partial \chi_1} (\sinh \chi \cos \gamma_1) = \cosh \chi, \quad (3.6)$$

$$\frac{\partial}{\partial \chi_2} (\sinh \chi \cos \gamma_1) = -\cosh \chi \cos \tilde{\theta}, \quad (3.7)$$

where

$$\cos \tilde{\theta} = \frac{\sin \gamma_1 \sin \gamma_2}{\cosh \chi} - \cos \gamma_1 \cos \gamma_2 = \frac{\cosh \chi_1 \cosh \chi_2 \cos \theta - \sinh \chi_1 \sinh \chi_2}{\cosh \chi_1 \cosh \chi_2 - \sinh \chi_1 \sinh \chi_2 \cos \theta}. \quad (3.8)$$

One can prove $|\cos \tilde{\theta}| \leq 1$ with this definition and $\theta \rightarrow \tilde{\theta}$ for the scale much less than the curvature scale, $\chi \ll |K|^{-2}$. We also use the derivatives of the radial part of the harmonic function $X_l(\nu, \chi)$, given by equation (B13), and the recursion relation, given by equation (B16). The explicit form of the radial part of the harmonic function X_l is presented in Appendix B, equations (B19)–(B23).

After straightforward but somewhat tedious algebra, using equations (3.3)–(3.8), (B13) and (B16), one obtains the spatial derivatives along the lines of sight as

$$\frac{\partial X_0}{\partial \chi_1} = \cos \gamma_1 X_1, \quad (3.9)$$

$$\frac{\partial^2 X_0}{\partial \chi_1^2} = X_0 - \frac{1}{3}(\nu^2 + 4)X_0 + \left(\cos^2 \gamma_1 - \frac{1}{3}\right) X_2, \quad (3.10)$$

$$\frac{\partial^2 X_0}{\partial \chi_1 \partial \chi_2} = -\cos \tilde{\theta} X_0 + \frac{1}{3} \cos \tilde{\theta} (\nu^2 + 4) X_0 + \left(\cos \gamma_1 \cos \gamma_2 + \frac{1}{3} \cos \tilde{\theta}\right) X_2, \quad (3.11)$$

$$\begin{aligned} \frac{\partial^3 X_0}{\partial \chi_1^2 \partial \chi_2} &= \cos \gamma_2 X_1 + \frac{1}{5} \left(2 \cos \gamma_1 \cos \tilde{\theta} - \cos \gamma_2\right) (\nu^2 + 4) X_1 \\ &\quad + \frac{1}{5} \left(2 \cos \gamma_1 \cos \tilde{\theta} + 5 \cos^2 \gamma_1 \cos \gamma_2 - \cos \gamma_2\right) X_3, \end{aligned} \quad (3.12)$$

$$\begin{aligned} \frac{\partial^4 X_0}{\partial \chi_1^2 \partial \chi_2^2} &= X_0 - \frac{2}{15} \left(4 + 3 \cos^2 \tilde{\theta}\right) (\nu^2 + 4) X_0 + \frac{1}{15} \left(1 + 2 \cos^2 \tilde{\theta}\right) (\nu^2 + 4)^2 X_0 \\ &\quad - \frac{1}{21} \left[4 - 6 \cos^2 \tilde{\theta} - 27 \left(\cos^2 \gamma_1 + \cos^2 \gamma_2\right) - 60 \cos \gamma_1 \cos \gamma_2 \cos \tilde{\theta}\right] X_2 \\ &\quad + \frac{1}{21} \left[2 + 4 \cos^2 \tilde{\theta} - 3 \left(\cos^2 \gamma_1 + \cos^2 \gamma_2\right) + 12 \cos \gamma_1 \cos \gamma_2 \cos \tilde{\theta}\right] (\nu^2 + 4) X_2 \\ &\quad + \frac{1}{35} \left[1 + 2 \cos^2 \tilde{\theta} - 5 \left(\cos^2 \gamma_1 + \cos^2 \gamma_2\right) + 20 \cos \gamma_1 \cos \gamma_2 \cos \tilde{\theta}\right. \\ &\quad \left.+ 35 \cos^2 \gamma_1 \cos^2 \gamma_2\right] X_4. \end{aligned} \quad (3.13)$$

Thus, $\widehat{R}_1 \widehat{R}_2 X_0(\nu, \chi)$ is expanded as follows:

$$\widehat{R}_1 \widehat{R}_2 X_0(\nu, \chi) = \sum_{n,l} c_l^{(n)}(\chi_1, \chi_2, \theta) \frac{(-1)^n X_l(\nu, \chi)}{\sinh^{2n-l} \chi (\nu^2 + 4)^n}, \quad (3.14)$$

where $(n, l) = (0, 0), (1, 0), (1, 1), (1, 2), (2, 0), (2, 1), (2, 2), (2, 3), (2, 4)$, and coefficients $c_l^{(n)}$ are given by

$$c_0^{(0)} = 1 + \frac{1}{3}(\beta_1 + \beta_2) + \frac{1}{15}\beta_1\beta_2 \left(1 + 2 \cos^2 \tilde{\theta}\right), \quad (3.15)$$

$$c_0^{(1)} = \left[\beta_1 + \beta_2 + \frac{2}{15}\beta_1\beta_2 \left(4 + 3 \cos \tilde{\theta}\right)\right] \sinh^2 \chi - \frac{1}{3}\beta_1\beta_2 \tilde{\alpha}_1 \tilde{\alpha}_2 \cos \tilde{\theta}, \quad (3.16)$$

$$c_1^{(1)} = \beta_1 \tilde{\alpha}_1 \cos \gamma_1 + \beta_2 \tilde{\alpha}_2 \cos \gamma_2 + \frac{1}{5}\beta_1\beta_2 \left[\tilde{\alpha}_1 \left(\cos \gamma_1 - 2 \cos \gamma_2 \cos \tilde{\theta}\right) + \tilde{\alpha}_2 \left(\cos \gamma_2 - 2 \cos \gamma_1 \cos \tilde{\theta}\right)\right], \quad (3.17)$$

$$c_2^{(1)} = \beta_1 \left(\cos^2 \gamma_1 - \frac{1}{3}\right) + \beta_2 \left(\cos^2 \gamma_2 - \frac{1}{3}\right) - \frac{1}{7}\beta_1\beta_2 \left[\frac{2}{3} + \frac{4}{3} \cos^2 \tilde{\theta} - \left(\cos^2 \gamma_1 + \cos^2 \gamma_2\right) + 4 \cos \gamma_1 \cos \gamma_2 \cos \tilde{\theta}\right], \quad (3.18)$$

$$c_0^{(2)} = \beta_1\beta_2 \left(\sinh^2 \chi - \tilde{\alpha}_1 \tilde{\alpha}_2\right) \sinh^2 \chi, \quad (3.19)$$

$$c_1^{(2)} = \beta_1\beta_2 \left(\tilde{\alpha}_1 \cos \gamma_1 + \tilde{\alpha}_2 \cos \gamma_2\right) \sinh^2 \chi, \quad (3.20)$$

$$c_2^{(2)} = \frac{2}{7}\beta_1\beta_2 \left[\cos^2 \tilde{\theta} - \frac{2}{3} + \frac{9}{2} \left(\cos^2 \gamma_1 + \cos^2 \gamma_2\right) + 10 \cos \gamma_1 \cos \gamma_2 \cos \tilde{\theta}\right] \sinh^2 \chi + \beta_1\beta_2 \tilde{\alpha}_1 \tilde{\alpha}_2 \left(\cos \gamma_1 \cos \gamma_2 + \frac{1}{3} \cos \tilde{\theta}\right), \quad (3.21)$$

$$c_3^{(2)} = \frac{1}{5}\beta_1\beta_2 \left[\tilde{\alpha}_1 \left(5 \cos \gamma_1 \cos^2 \gamma_2 - \cos \gamma_1 + 2 \cos \gamma_2 \cos \tilde{\theta}\right) + \tilde{\alpha}_2 \left(5 \cos \gamma_2 \cos^2 \gamma_1 - \cos \gamma_2 + 2 \cos \gamma_1 \cos \tilde{\theta}\right)\right], \quad (3.22)$$

$$c_4^{(2)} = \frac{1}{7}\beta_1\beta_2 \left[\frac{1}{5} + \frac{2}{5} \cos^2 \tilde{\theta} - \left(\cos^2 \gamma_1 + \cos^2 \gamma_2\right) + 4 \cos \gamma_1 \cos \gamma_2 \cos \tilde{\theta} + 7 \cos^2 \gamma_1 \cos^2 \gamma_2\right], \quad (3.23)$$

where

$$\tilde{\alpha}_1(\chi_1, \chi) = \alpha(\chi_1) \sinh \chi = \sinh \chi \frac{\cosh \chi_1}{\sinh \chi_1} \left(2 + \frac{\partial \ln(D_1 f_1 \Phi_1)}{\partial \ln \sinh \chi_1}\right), \quad (3.24)$$

$$\tilde{\alpha}_2(\chi_2, \chi) = \alpha(\chi_2) \sinh \chi = \sinh \chi \frac{\cosh \chi_2}{\sinh \chi_2} \left(2 + \frac{\partial \ln(D_2 f_2 \Phi_2)}{\partial \ln \sinh \chi_2}\right), \quad (3.25)$$

and $\beta_1 = \beta(z_1)$, $\beta_2 = \beta(z_2)$, $f_1 = f(z_1)$, $f_2 = f(z_2)$, $\Phi_1 = \Phi(\chi_1)$, $\Phi_2 = \Phi(\chi_2)$. Since these coefficients do not depend on ν , the correlation function in redshift space of equation (2.32)

finally reduces to

$$\xi(\mathbf{x}_1, \mathbf{x}_2) = b_1 b_2 D_1 D_2 \sum_{n,l} c_l^{(n)}(\chi_1, \chi_2, \theta) \Xi_l^{(n)}(\chi), \quad (3.26)$$

where

$$\Xi_l^{(n)}(\chi) = \frac{(-1)^n}{\sinh^{2n-l} \chi} \int \frac{\nu^2 d\nu}{2\pi^2} \frac{X_l(\nu, \chi)}{(\nu^2 + 4)^n} S(\nu). \quad (3.27)$$

In the left panel of Figure 2, some examples of the function $\Xi_l^{(n)}(\chi)$ for an open model are plotted. The CDM-type transfer function (Bardeen et al. 1986) is adopted and the primordial power spectrum on large scales is assumed to be “scale invariant”, which corresponds to constant fluctuations in the gravitational potential per logarithmic interval in wavenumber (Lyth & Stewart 1990; Ratra & Peebles 1994; White & Bunn 1995):

$$S(\nu) \propto \frac{(\nu^2 + 4)^2}{\nu(\nu^2 + 1)} T^2 (|K|^{1/2} \nu / \Gamma), \quad (3.28)$$

where

$$T(p) = \frac{\ln(1 + 2.34p)}{2.34p} \left[1 + 3.89p + (16.1p)^2 + (5.46p)^3 + (6.71p)^4 \right]^{-1/4}, \quad (3.29)$$

and the shape parameter is set $\Gamma/(h^{-1}\text{Mpc} = 0.2)$, which corresponds to $\Gamma = 6 \times 10^2 (cH_0^{-1})^{-1}$ in our unit system. On scales smaller than Horizon scale, $\nu \gg 1$, the power spectrum (3.28) reduces to usual CDM-type power spectrum with Harrison-Zel’dovich primordial spectrum.

The set of equations (3.15)–(3.27) is our final formula for the correlation function in redshift space which takes into account the light-cone, and spatial-curvature effect *without* distant-observer approximation.

3.2. A Flat Universe

In a flat universe ($K = 0$), the correlation function in real space is given by equation (B51):

$$\xi(\chi) = \int \frac{\nu^2 d\nu}{2\pi^2} X_0(\nu, \chi) S(\nu), \quad (3.30)$$

where

$$X_0 = \frac{\sin \nu \chi}{\nu \chi}. \quad (3.31)$$

We can repeat the similar calculation of the previous subsection for a flat universe ($K = 0$). The corresponding formula can also be used if we only consider a nearby universe where the separation χ and the distances χ_1, χ_2 are much smaller than the curvature scale, $|K|^{-1/2}$, which roughly corresponds to the horizon scale.

The calculation for a flat universe is performed similarly as in the previous subsection, or alternatively, we can also obtain the formula in a flat limit from the formula for an open universe, taking the limit $\chi_1, \chi_2, \chi \rightarrow 0, \nu \rightarrow \infty$, with $\nu\chi$ fixed. Anyway, the equation (3.3) reduces to the one in Euclidean geometry:

$$\chi^2 = \chi_1^2 + \chi_2^2 - 2\chi_1\chi_2 \cos \theta. \quad (3.32)$$

The meaning of γ_1 and γ_2 is the same, and they are explicitly given by

$$\cos \gamma_1 = \frac{\chi_1 - \chi_2 \cos \theta}{\chi}, \quad \cos \gamma_2 = \frac{\chi_2 - \chi_1 \cos \theta}{\chi}. \quad (3.33)$$

The variable $\tilde{\theta}$ in flat universe, defined by equation (3.8) for the case of an open universe, reduces to θ , the angle between lines of sight of \mathbf{x}_1 and \mathbf{x}_2 with respect to the observer.

Thus, the correlation function in redshift space is given by equation (3.26) where the coefficients $c_i^{(n)}$ in a flat universe are

$$c_0^{(0)} = 1 + \frac{1}{3}(\beta_1 + \beta_2) + \frac{1}{15}\beta_1\beta_2 (1 + 2 \cos^2 \theta), \quad (3.34)$$

$$c_0^{(1)} = -\frac{1}{3}\beta_1\beta_2\tilde{\alpha}_1\tilde{\alpha}_2 \cos \theta, \quad (3.35)$$

$$c_1^{(1)} = \beta_1\tilde{\alpha}_1 \cos \gamma_1 + \beta_2\tilde{\alpha}_2 \cos \gamma_2 + \frac{1}{5}\beta_1\beta_2 [\tilde{\alpha}_1 (\cos \gamma_1 - 2 \cos \gamma_2 \cos \theta) + \tilde{\alpha}_2 (\cos \gamma_2 - 2 \cos \gamma_1 \cos \theta)], \quad (3.36)$$

$$c_2^{(1)} = \beta_1 \left(\cos^2 \gamma_1 - \frac{1}{3} \right) + \beta_2 \left(\cos^2 \gamma_2 - \frac{1}{3} \right) - \frac{1}{7}\beta_1\beta_2 \left[\frac{2}{3} + \frac{4}{3} \cos^2 \theta - (\cos^2 \gamma_1 + \cos^2 \gamma_2) + 4 \cos \gamma_1 \cos \gamma_2 \cos \theta \right], \quad (3.37)$$

$$c_0^{(2)} = 0, \quad (3.38)$$

$$c_1^{(2)} = 0, \quad (3.39)$$

$$c_2^{(2)} = \beta_1\beta_2\tilde{\alpha}_1\tilde{\alpha}_2 \left(\cos \gamma_1 \cos \gamma_2 + \frac{1}{3} \cos \theta \right), \quad (3.40)$$

$$c_3^{(2)} = \frac{1}{5}\beta_1\beta_2 \left[\tilde{\alpha}_1 (5 \cos \gamma_1 \cos^2 \gamma_2 - \cos \gamma_1 + 2 \cos \gamma_2 \cos \theta) + \tilde{\alpha}_2 (5 \cos \gamma_2 \cos^2 \gamma_1 - \cos \gamma_2 + 2 \cos \gamma_1 \cos \theta) \right], \quad (3.41)$$

$$c_4^{(2)} = \frac{1}{7}\beta_1\beta_2 \left[\frac{1}{5} + \frac{2}{5} \cos^2 \theta - (\cos^2 \gamma_1 + \cos^2 \gamma_2) + 4 \cos \gamma_1 \cos \gamma_2 \cos \theta \right]$$

$$+ 7 \cos^2 \gamma_1 \cos^2 \gamma_2 \Big], \quad (3.42)$$

where

$$\tilde{\alpha}_1(\chi_1, \chi) = \alpha(\chi_1)\chi = \frac{\chi}{\chi_1} \left(2 + \frac{\partial \ln(D_1 f_1 \Phi_1)}{\partial \ln \chi_1} \right), \quad (3.43)$$

$$\tilde{\alpha}_2(\chi_2, \chi) = \alpha(\chi_2)\chi = \frac{\chi}{\chi_2} \left(2 + \frac{\partial \ln(D_2 f_2 \Phi_2)}{\partial \ln \chi_2} \right), \quad (3.44)$$

The corresponding equation of (3.27) is

$$\Xi_l^{(n)}(\chi) = \frac{(-1)^n}{\chi^{2n-l}} \int \frac{\nu^2 d\nu}{2\pi} \frac{X_l(\nu, \chi)}{\nu^{2n}} S(\nu) = \frac{(-1)^{n+l}}{x^{2n-l}} \int \frac{k^2 dk}{2\pi^2} \frac{j_l(kx)}{k^{2n-l}} P(k). \quad (3.45)$$

In the middle panel of Figure 2, some examples of the function $\Xi_l^{(n)}(\chi)$ for a flat model are plotted for scale invariant primordial power spectrum with CDM-type transfer function:

$$S(\nu) \propto \nu T^2(\nu/\Gamma), \quad (3.46)$$

where we again set the shape parameter $\Gamma/(h^{-1}\text{Mpc}) = 0.2$.

Alternatively, the coefficients $c_l^{(n)}$ can also be represented by using variables $\gamma \equiv \gamma_2 + \theta$ and $\theta_h = \theta/2$. These variables are introduced in Szalay, Matsubara & Landy (1998) in a calculation of wide-angle effects of nearby universe ($z \ll 1$), except that their original definition of γ is $\pi - \gamma$, instead. The meaning of γ is the angle between $\mathbf{x}_2 - \mathbf{x}_1$ and a symmetry axis that halves the angle θ .

With these new variables, equations (3.34)–(3.42) are transformed as

$$c_0^{(0)} = 1 + \frac{1}{3}(\beta_1 + \beta_2) + \frac{1}{5}\beta_1\beta_2 - \frac{8}{15}\beta_1\beta_2 \cos^2 \theta_h \sin^2 \theta_h, \quad (3.47)$$

$$c_0^{(1)} = -\frac{1}{3}\beta_1\beta_2\tilde{\alpha}_1\tilde{\alpha}_2 \cos 2\theta_h, \quad (3.48)$$

$$\begin{aligned} c_1^{(1)} = & \left[(\beta_1\tilde{\alpha}_1 + \beta_2\tilde{\alpha}_2) + \frac{1}{5}\beta_1\beta_2(\tilde{\alpha}_1 + \tilde{\alpha}_2) (3 - 4 \cos^2 \theta_h) \right] \sin \theta_h \sin \gamma \\ & - \left[(\beta_1\tilde{\alpha}_1 - \beta_2\tilde{\alpha}_2) + \frac{1}{5}\beta_1\beta_2(\tilde{\alpha}_1 - \tilde{\alpha}_2) (3 - 4 \sin^2 \theta_h) \right] \cos \theta_h \cos \gamma, \end{aligned} \quad (3.49)$$

$$\begin{aligned} c_2^{(1)} = & \left[\frac{2}{3}(\beta_1 + \beta_2) + \frac{4}{7}\beta_1\beta_2 \right] \cos 2\theta_h P_2(\cos \gamma) \\ & + \frac{1}{3} \left[(\beta_1 + \beta_2) - \frac{2}{7}\beta_1\beta_2 + \frac{8}{7}\beta_1\beta_2 \sin^2 \theta_h \right] \sin^2 \theta_h \\ & - 2(\beta_1 - \beta_2) \cos \theta_h \sin \theta_h \cos \gamma \sin \gamma, \end{aligned} \quad (3.50)$$

$$c_0^{(2)} = 0, \quad (3.51)$$

$$c_1^{(2)} = 0, \quad (3.52)$$

$$c_2^{(2)} = \frac{1}{3}\beta_1\beta_2\tilde{\alpha}_1\tilde{\alpha}_2\left(\sin^2\theta_h - 2P_2(\cos\gamma)\right), \quad (3.53)$$

$$c_3^{(2)} = -\frac{1}{5}\beta_1\beta_2\left\{(\tilde{\alpha}_1 + \tilde{\alpha}_2)\sin\theta_h\left[\cos^2\theta_h P_1(\sin\gamma) - 2P_3(\sin\gamma)\right] - (\tilde{\alpha}_1 - \tilde{\alpha}_2)\cos\theta_h\left[\sin^2\theta_h P_1(\cos\gamma) - 2P_3(\cos\gamma)\right]\right\}, \quad (3.54)$$

$$c_4^{(2)} = \frac{1}{7}\beta_1\beta_2\left[\frac{8}{5}P_4(\cos\gamma) - \frac{4}{3}\sin^2\theta_h P_2(\cos\gamma) - \frac{1}{15}(4 - 9\sin^2\theta_h)\sin^2\theta_h\right], \quad (3.55)$$

where $P_l(x)$ is the Legendre function.

3.3. A Closed Universe

In a closed universe ($K > 0$), the correlation function in real space is given by the equation (B52):

$$\xi(\chi) = \sum_{\nu=3}^{\infty} \frac{\nu^2}{2\pi^2} X_0(\nu, \chi) S(\nu), \quad (3.56)$$

where

$$X_0 = \frac{\sin\nu\chi}{\nu\sin\chi}. \quad (3.57)$$

Repeating the similar calculation as in an open universe, or formally putting $\chi \rightarrow i\chi$, $\chi_1 \rightarrow i\chi_1$, $\chi_2 \rightarrow i\chi_2$ and $\nu \rightarrow -i\nu$ in the calculation for an open universe, we obtain the formula for a closed universe. In this subsection, we just summarize the difference of the formula from the case of an open universe.

The corresponding equation (3.3) in a closed universe is

$$\cos\chi = \cos\chi_1\cos\chi_2 + \sin\chi_1\sin\chi_2\cos\theta, \quad (3.58)$$

The meaning of γ_1 and γ_2 is unchanged and they are given by

$$\cos\gamma_1 = \frac{1}{\sin\chi}(\sin\chi_1\cos\chi_2 - \cos\chi_1\sin\chi_2\cos\theta), \quad (3.59)$$

$$\cos\gamma_2 = \frac{1}{\sin\chi}(\cos\chi_1\sin\chi_2 - \sin\chi_1\cos\chi_2\cos\theta) \quad (3.60)$$

The variable $\tilde{\theta}$ in a closed universe is defined by

$$\cos\tilde{\theta} = \frac{\sin\gamma_1\sin\gamma_2}{\cos\chi} - \cos\gamma_1\cos\gamma_2 = \frac{\cos\chi_1\cos\chi_2\cos\theta + \sin\chi_1\sin\chi_2}{\cos\chi_1\cos\chi_2 + \sin\chi_1\sin\chi_2\cos\theta}. \quad (3.61)$$

Then the form of the coefficients $c_l^{(n)}$ of equation (3.15)–(3.23) is almost the same, and we do not repeat the formula here. The only difference is that $\sinh \chi$ should be replaced by $\sin \chi$, and the definition of $\tilde{\alpha}$ is changed as

$$\tilde{\alpha}_1(\chi_1, \chi) = \alpha(\chi_1) \sin \chi = \sin \chi \frac{\cos \chi_1}{\sin \chi_1} \left(2 + \frac{\partial \ln(D_1 f_1 \Phi_1)}{\partial \ln \sin \chi_1} \right), \quad (3.62)$$

$$\tilde{\alpha}_2(\chi_2, \chi) = \alpha(\chi_2) \sin \chi = \sin \chi \frac{\cos \chi_2}{\sin \chi_2} \left(2 + \frac{\partial \ln(D_2 f_2 \Phi_2)}{\partial \ln \sin \chi_2} \right). \quad (3.63)$$

The formula for a closed universe is also given by the equation (3.26) where the definition of $\Xi_l^{(n)}$ is replaced by

$$\Xi_l^{(n)}(\chi) = \frac{1}{\sin^{2n-l} \chi} \sum_{\nu=3}^{\infty} \frac{\nu^2}{2\pi^2} \frac{X_l(\nu, \chi)}{(\nu^2 - 4)^n} S(\nu). \quad (3.64)$$

In the right panel of Figure 2, some examples of the function $\Xi_l^{(n)}(\chi)$ are plotted for a closed model. As in the open case, the primordial power spectrum on large scales is assumed to be “scale invariant”, which corresponds to constant fluctuations in the gravitational potential per logarithmic interval in wavenumber (White & Scott 1996):

$$S(\nu) \propto \frac{(\nu^2 - 4)^2}{\nu(\nu^2 - 1)} T^2 (|K|^{1/2} \nu / \Gamma). \quad (3.65)$$

where we again set the shape parameter as $\Gamma/(h^{-1}\text{Mpc}) = 0.2$

3.4. Recovery of the Known Formulas of the Redshift Distortions of the Correlation Function

It is an easy exercise to derive the previously known formulas of the redshift distortions of the correlation function from our general formula. We illustrate how our formula reduces to the known formulas by taking appropriate limits. Here we consider two approximations, $\chi \ll \chi_1, \chi_2$ and/or $z \ll 1$. The first approximation corresponds to the distant observer approximation. In this approximation, the distance between two points is much smaller than the distances of these points from the observer. The second approximation corresponds to only considering the nearby universe. The redshift distortion formulas known so far are restricted in these cases.

First of all, consider a limit $\chi \ll \chi_1, \chi_2$, with γ_1, γ_2 fixed. We also set $\beta_1 = \beta_2 = \beta$, and the distance between the two points χ is much smaller than the curvature scale. Then

irrespective to the spatial curvature, $\theta, \tilde{\theta} \rightarrow 0$, and $\gamma_2 \rightarrow \pi - \gamma_1 \equiv \gamma$. Both the coefficients (3.15)–(3.23), and (3.34)–(3.42) reduce to

$$c_0^{(0)} = 1 + \frac{2}{3}\beta + \frac{1}{5}\beta^2 \quad (3.66)$$

$$c_2^{(1)} = \left(\frac{4}{3}\beta + \frac{4}{7}\beta^2\right) P_2(\cos \gamma), \quad (3.67)$$

$$c_4^{(2)} = \frac{8}{35}\beta^2 P_4(\cos \gamma), \quad (3.68)$$

and all the other coefficients are zero. These coefficients are equivalent to the result that Hamilton (1992) derived in $z \rightarrow 0$ limit with distant observer approximation, which is a direct Fourier transform of Kaiser’s original form in Fourier space (Kaiser 1987). For finite z , the equivalent result is obtained by Matsubara & Suto (1996) for correlation function and Ballinger, Peacock & Heavens (1996) for power spectrum [see also Nakamura, Matsubara & Suto (1998) de Laix & Starkman (1998), Nair (1999)]. All these previous studies are based on the distant observer approximation, and our general formula correctly has the limit of these cases.

The wide-angle effects on the redshift distortion of the correlation function without distant observer approximation is already derived for nearby universe, $z \ll 0$ by Szalay, Matsubara & Landy (1998), and Bharadwaj (1999) also derived the equivalent result with another parameterization. It is easy to see that our general results have the correct limit of Szalay et al. (1998). In the limit $z \rightarrow 0$ the geometry reduces to be flat case, and, in fact, equations (3.47)–(3.55) with $\beta_1 = \beta_2 \equiv \beta$ in that limit is completely equivalent to the result of Szalay et al. (1998) after correcting their typographical errors³, noting the minor difference of the definition that γ and $\Xi_l^{(n)}$ here correspond to $\pi - \gamma$ and $(-1)^{n+l} x^{-2n+l} \xi_l^{(2n-l)}$ in Szalay et al. (1998), respectively.

4. THE REDSHIFT DISTORTIONS AND THE SPATIAL CURVATURE OF THE UNIVERSE

It is well known that the redshift distortions of the correlation function for nearby universe are good probes of the density parameter modulo bias factor at present time, $\beta_0 = \Omega_0^{0.6}/b_0$. The parameter β_0 is called as the redshift distortion parameter of nearby universe. Redshift distortions of nearby universe do not depend on spatial curvature almost

³The factor 4/15 in the last term of their equation (15) should be replaced by 8/15 and the left hand side of their equation (20) should be replaced by $1/3 \cdot \alpha_1 \alpha_2 \beta^2 \cos 2\theta$.

at all, because the redshift distortions of nearby universe are purely caused by the peculiar velocity field, which is almost independent on the spatial curvature. However, the redshift distortions at high redshifts, say $z \gtrsim 1$ in a quasar catalog, definitely depend on the spatial curvature of the universe and is called as cosmological redshift distortion. Matsubara & Suto (1996) explicitly show the dependence of the cosmological distortion of the correlation function on cosmological parameters, employing the distant observer approximation. To probe more properly the spatial curvature with cosmological distortions, it is not desirable to rely on the distant observer approximation.

In this section, we numerically calculate the formula obtained in the previous section for several models, concentrating on geometrical effects. We plot the correlation function in directly observable velocity space. In the following, the shape parameter for the CDM-type transfer function is fixed to $\Gamma = 6 \times 10^2$ in our unit system, which corresponds to $\Gamma/(h^{-1}\text{Mpc}) = 0.2$, in spite of the fact that CDM model predict $\Gamma/(h^{-1}\text{Mpc}) = \Omega_0 h$. We fix the spectrum simply because we are interested in the pure distortion effects on the difference among the models, while the difference of the shape of the underlying power spectrum is less interested in here. The primordial spectrum is assumed to be “scale invariant”, which corresponds to constant fluctuations in the gravitational potential per logarithmic interval in wavenumber, equations (3.28), (3.46) and (3.65). For simplicity, we assume no bias, $b = 1$ and also assume $\alpha = 0$. The latter assumption corresponds to the case $Df\Phi(\chi) \propto (\sinh \chi)^{-2}$, χ^{-2} , and $(\sin \chi)^{-2}$, for open, flat, and closed models, respectively. Although this form of selection function is not physically motivated, it is not so unrealistic for merely illustrative purpose. In actual application, the selection function is individually determined for each redshift survey.

Figures 3–6 show the contour plots of the correlation function. Each figure consists of 12 panels. In each figure, from top to bottom, the cosmological models are $(\Omega_0, \lambda_0) = (1, 0), (0.2, 0.8), (0.2, 0)$, respectively, which we call STD, FLAT, and OPEN models. From left to right, the redshifts of the first points are $z = 0.1, 0.3, 1.0, 3.0$, respectively.

In Figures 3 and 4, the correlation function with the purely geometrical distortions is plotted for an illustrative purpose, assuming there are no peculiar velocities at all, by setting $\beta = 0$ in our formula. The first point, \mathbf{x}_1 of equation (3.26), is at the center on the y-axis in each figures. The contour plot show the value of correlation function depending on the position of the second point \mathbf{x}_2 . In Figure 3, the observer is located at the origin $(0, 0)$ and the global distortions are shown. In Figure 4, the scale of z around the first object is fixed, and the observer is located at $(0, -z_1)$, outside the plots.

For lower redshifts, $z = 0.1, 0.3$, the geometrical distortion is not significant. For higher

redshifts, $z = 1.0, 3.0$, due to the nonlinear relations of redshift and comoving distance, the contours are elongated to the direction of line of sight in all three models. The extent of the elongation for STD and OPEN models are similar, but the elongation for FLAT model is smaller than other models. This is because the acceleration nature due to the cosmological constant squashes the z -space along the line of sight (Alcock & Paczyński 1979).

In Figures 5 and 6, the correlation function in redshift space is plotted, taking into account the velocity distortions. As in Figures 3 and 4, the observer is located $(0, 0)$ and $(0, -z_1)$, respectively.

For lower redshifts, the redshift distortions are mainly from peculiar velocity fields, which depends only on the density parameter Ω_0 . Thus, STD model can be discriminated from other models by correlation function of lower redshifts, but FLAT and OPEN models are similar. For higher redshifts, FLAT and OPEN models become different because of the squashing by the cosmological constant.

To illustrate the difference among profiles of correlation function in redshift space for different models and different redshifts, we define the parallel correlation function $\xi_{\parallel}(z_{\parallel}; z)$ and perpendicular correlation function $\xi_{\perp}(z_{\perp}; z)$ at given z . In terms of the correlation function in redshift space $\xi^{(s)}(z_1, z_2, \theta)$ they are defined by

$$\xi_{\parallel}(z_{\parallel}; z) = \xi^{(s)}\left(z - \frac{z_{\parallel}}{2}, z + \frac{z_{\parallel}}{2}, 0\right), \quad (4.1)$$

$$\xi_{\perp}(z_{\perp}; z) = \xi^{(s)}\left(z, z, \text{Arccos}\left[1 - \frac{z_{\perp}^2}{2z^2}\right]\right). \quad (4.2)$$

The geometrical meaning of the definition of the parallel redshift interval z_{\parallel} and the perpendicular redshift interval z_{\perp} are illustrated in Figure 7. As seen from the Figure 5 or 6, these sections of correlation function are supposed to be maximally distorted in opposite direction, and that is the reason why we introduce them for illustrations. These functions are the generalization of the similar functions introduced by Matsubara & Suto (1996) in the case of distant observer approximation.

In Figure 8, those parallel and perpendicular correlation functions are plotted for STD, FLAT, and OPEN models. The correlation function in real space is normalized as $\sigma_8 = 1$. One can notice that while the perpendicular correlation functions are not significantly different among three models, the parallel correlation functions are quite different. For lower redshifts, profiles of the parallel correlation function for the FLAT and OPEN models are similar as usual. For higher redshifts, the relative amplitude of ξ_{\parallel} compared to ξ_{\perp} in the OPEN model is higher than that in the FLAT model. In addition to that, the zero-crossing point of ξ_{\parallel} in the OPEN model is larger than that in the FLAT model. Those tendencies are both explained by the cosmological-constant squashing, because the squashing shifts

the profile toward small scales, or left. Even if the determination of the zero-crossing point of ξ_{\parallel} is observationally difficult, the former effect on the relative amplitude is a promising one to discriminate the spatial curvature by the observation of redshift distortions.

The distant observer approximation has been widely used in the analyses of galaxy redshift surveys. With our general formula, we can figure out when this approximation is valid and when it is not. The distant observer approximation of the two-point correlation function is derived by Hamilton (1992) for a nearby universe, $z \ll 1$. Matsubara & Suto (1996) generalize his formula to arbitrary redshifts, in which the distant observer approximation is still adopted. In Figure 9, we plot the ratio of the value of those two previous formulas and that of our formula. We choose the geometry of the two points as follows: we fix the separation $z_{12} \equiv (z_1^2 + z_2^2 - 2z_1z_2 \cos \theta)^{1/2}$ of the two points in velocity space. The angle γ_z between the symmetric line which halves the lines of sight and the line between the two points is also fixed. The meaning of the angle γ_z is the inclination of z_{12} relative to the line of sight in velocity space. Explicitly, γ_z is given by $\tan \gamma_z = (z_1 + z_2)|z_1 - z_2|^{-1} \tan(\theta/2)$. The angle θ between the lines of sight is varied in the figure. We plot the cases, $z_{12} = 0.003, 0.006, 0.012, 0.024$, and $\gamma_z = 10^\circ, 45^\circ, 80^\circ$. There is some irregular behavior that corresponds to the zero crossings of the correlation function.

The Hamilton’s formula (thin lines) is valid when the separation z_{12} is not so large. The reason why the Hamilton’s formula deviate even in small angles is that when the angle is small enough, the redshift becomes large, and the evolutionary and geometrical effects are not negligible. In fact, the formula of Matsubara & Suto (thick lines) is perfectly identical to our general formula when the angle is small.

The validity region of the distant observer approximation depends on the inclination angle γ_z . However, one can conservatively estimate the validity region as $\theta \lesssim 10^\circ$. One can use $\theta \sim 20^\circ$ for some cases, while the blind application of the approximation for $\theta \sim 30^\circ$ can cause over 100% error.

5. CONCLUSIONS

In this paper we have derived for the first time the unified formula of the correlation function in redshift space in linear theory, which simultaneously includes wide-angle effects and the cosmological redshift distortions. The effects of the spatial curvature both on geometry and on fluctuation spectrum are properly taken into account, and our formula applies to an arbitrary Friedman-Lemaître universe.

The distant observer approximation by Matsubara & Suto (1996), which is a

generalization of the work by Hamilton (1992), can be used when the angle θ between the lines of sight is less than 10° . Beyond that range, our formula provides a unique one for the correlation function in redshift space with geometrical distortions.

The correlation function in redshift space is uniquely determined if the cosmological parameters Ω_0 , λ_0 , the power spectrum $P(k)$ and bias evolution $b(z)$ is specified. The Hubble constant does not affect the correlation function, provided that we do not adopt a specific model to the power spectrum and/or to the bias evolution which may depend on Hubble constant. Our formula predicts the correlation function for a fixed model of these variables and one can test any model by directly comparing the correlation function of the data and of the theoretical prediction in redshift space.

Now we comment on some caveats for our formula. First, when we try to apply our formula to the scale $\lesssim 20h^{-1}\text{Mpc}$, what apparently lacks in our formula is the finger-of-God effect, or the nonlinear smearing of the correlation along the line of sight. While it is still difficult to analytically include this effect into our formula, one can phenomenologically evaluate the effect by numerically smearing the formula along the line of sight. Second, our formula does not include the Sachs-Wolfe and gravitational lensing effects. The Sachs-Wolfe effect could affect our formula only on scales comparable to Hubble distance where the correlation function is too small to be practically detectable, as discussed in section 2.1. However, it is possible that the gravitational lensing effect affects the observable correlation function for $z \gtrsim 1$. In which case, one should add correction terms to our formula. Even so, our formula for $z \lesssim 1$ would not be affected by those terms and still corresponds to the observable quantity. Those correction terms by gravitational lensing will be given in a future paper. Third, our formula assumes the selection function uncorrelated to the density fluctuations. In addition, the precise form of the selection function is practically difficult to determine. If the luminosities and/or the surface brightnesses are correlated to density fluctuations, it can mimic the large-scale structure.

It could be the case that one can blindly seek the models of cosmological quantities, Ω_0 , λ_0 , $P(k)$, and $b(z)$. Each quantity has different effects on the correlation function in redshift space. Roughly speaking, the cosmological parameters Ω_0 and λ_0 mostly affect the distortions of the contour of the correlation function, the power spectrum $P(k)$ mostly affects the profile of the correlation function, and the bias evolution mostly affects the z -dependence of the amplitude. Since all the pairs of the objects in the redshift survey can be used, we can expect that those quantities are determined with small errors by performing proper likelihood analysis, such as the Karhunen-Loève mode decomposition (Vogele & Szalay 1996; Matsubara, Szalay & Landy 1999). The application of the formula to the actual data is a straightforward task. We believe the formula presented in this paper is one

of the most fundamental theoretical tools in understanding the data of the deep redshift surveys.

I wish to thank Alex Szalay, Naoshi Sugiyama and Yasushi Suto for stimulating discussions. This work was supported by JSPS Postdoctoral Fellowships for Research Abroad.

APPENDIX A

GAUGE-INVARIANT EVOLUTION EQUATIONS FOR THE DENSITY CONTRAST AND THE VELOCITY FIELD

In this appendix, we review the derivation of the equations of motion for the density contrast and the velocity field in the general relativistic context. We assume the matter is pressureless, perfect fluid, and the background metric is given by homogeneous, isotropic FLRW metric. For the perturbed Einstein equation,

$$\delta G^\mu{}_\nu = 8\pi G \delta T^\mu{}_\nu, \quad (\text{A1})$$

Bardeen (1980) introduced the gauge-invariant formalism. Here, we briefly review the formalism in the case of pressureless fluid, and derive relevant equations for our purpose, i.e., equations to relate the density contrast and the velocity field. In this appendix, we use the conformal time τ defined by $d\tau = dt/a$, so that the metric is given by

$$ds^2 = a^2(\tau) \left(-d\tau^2 + \gamma_{ij} dx^i dx^j \right), \quad (\text{A2})$$

in the coordinates (τ, x^i) . A prime denotes differentiation with respect to the conformal time.

The perturbations are classified into scalar, vector, and tensor types. The scalar perturbations are expanded by the complete set of scalar harmonics $Q(x^i)$ satisfying the Helmholtz equation

$$(\Delta + q^2)Q = 0, \quad (\text{A3})$$

where $\Delta = \nabla^i \nabla_i$ is the Laplacian and ∇_i is the three-dimensional covariant derivative with respect to the metric γ_{ij} . The explicit form of each mode of this solution is given in Appendix B. In the following, the indices to distinguish different modes are omitted and each mode function is represented by Q .

For each mode, the scalar perturbations in the metric (A2) are defined by

$$h_{00} = -2a^2 A(\tau) Q, \quad (\text{A4})$$

$$h_{0i} = -a^2 B(\tau) Q_{,i}, \quad (\text{A5})$$

$$h_{ij} = 2a^2 [H_L(\tau) Q \gamma_{ij} + H_T(\tau) Q_{,ij}], \quad (\text{A6})$$

where

$$Q_{,i} = -\frac{1}{q} \nabla_i Q, \quad (\text{A7})$$

$$Q_{,ij} = \frac{1}{q^2} \nabla_i \nabla_j Q + \frac{1}{3} \gamma_{ij} Q. \quad (\text{A8})$$

The three-velocity w^i associated with four-velocity u^μ is represented by

$$w^i = \frac{u^i}{u^0} = V(\tau)Q^i, \quad (\text{A9})$$

and to first order the normalization $u_\mu u^\mu = -1$ gives

$$u^0 = \frac{1 - A(\tau)Q}{a}. \quad (\text{A10})$$

The pressureless energy-momentum tensor is given by $T^\mu_\nu = \rho u^\mu u_\nu$, thus, the scalar perturbations in the pressureless energy-momentum tensor are

$$\delta T^0_0 = -\bar{\rho}\Delta(\tau)Q, \quad (\text{A11})$$

$$\delta T^0_j = \bar{\rho}[V(\tau) - B(\tau)]Q_j, \quad (\text{A12})$$

$$\delta T^i_j = 0. \quad (\text{A13})$$

In terms of the gauge-dependent variables A , B , H_L , H_T , V , and Δ , Bardeen (1980) defined gauge invariant combinations:

$$\Phi_A = A + \frac{1}{q}B' + \frac{1}{q}\frac{a'}{a}B - \frac{1}{q^2}\left(H_T'' + \frac{a'}{a}H_T'\right), \quad (\text{A14})$$

$$\Phi_H = H_L + \frac{1}{3}H_T + \frac{1}{q}\frac{a'}{a}B - \frac{1}{q^2}\frac{a'}{a}H_T', \quad (\text{A15})$$

$$\delta = \Delta + \frac{3}{q}\frac{a'}{a}(V - B), \quad (\text{A16})$$

$$V_s = V - \frac{1}{q}H_T'. \quad (\text{A17})$$

The perturbation equation (A1) for these scalar gauge-invariant variables are given by Bardeen (1980):

$$(q^2 - 3K)\Phi_H = 4\pi G a^2 \bar{\rho} \delta, \quad (\text{A18})$$

$$\Phi_A + \Phi_H = 0, \quad (\text{A19})$$

$$V_s' + \frac{a'}{a}V_s = q\Phi_A, \quad (\text{A20})$$

$$\delta' + (q^2 - 3K)\frac{1}{q}V_s = 0. \quad (\text{A21})$$

We define new variables $\psi = -a^{-1}q^{-1}V_s$ and $\Phi = a^{-2}\Phi_A$. After superposing the modes of the above equations, we obtain

$$\dot{\delta} + (\Delta + 3K)\psi = 0, \quad (\text{A22})$$

$$\dot{\psi} + 2H\psi + \Phi = 0, \quad (\text{A23})$$

$$(\Delta + 3K)\Phi = \frac{3}{2}H^2\Omega\delta, \quad (\text{A24})$$

where a dot denotes the differentiation with respect to the proper time, d/dt , and Δ is the Laplacian on FLRW metric, equation (B1), This is the complete set of equations to treat the scalar perturbations.

The velocity w^i corresponds to $dx^i/d\tau = a dx^i/dt = a v^i$, and the equation (A9) suggests $w^i = a \nabla^i \psi$, so that $v^i = \nabla^i \psi$, i.e., ψ is the velocity potential and represents the longitudinal part of the velocity v^i . The transverse part of v^i belongs to the vector perturbations.

The vector perturbations are expanded by the divergenceless vector harmonics $Q_i^{(1)}$ satisfying

$$(\Delta + q^2)Q_i^{(1)} = 0, \quad (\text{A25})$$

$$\nabla^i Q_i^{(1)} = 0. \quad (\text{A26})$$

For each mode, the vector perturbations are given by

$$h_{00} = 0, \quad (\text{A27})$$

$$h_{0i} = -a^2 B^{(1)}(\tau) Q_i^{(1)}, \quad (\text{A28})$$

$$h_{ij} = 2a^2 H_T^{(1)}(\tau) Q_{ij}^{(1)}, \quad (\text{A29})$$

where

$$Q_{ij}^{(1)} = -\frac{1}{2q} [\nabla_i Q_j^{(1)} + \nabla_j Q_i^{(1)}]. \quad (\text{A30})$$

The vector perturbations in the three-velocity are

$$w^i = \frac{u^i}{u^0} = V^{(1)}(\tau) Q^i, \quad (\text{A31})$$

and in the energy momentum tensor are

$$\delta T^0_0 = 0, \quad (\text{A32})$$

$$\delta T^0_j = \bar{\rho} [V^{(1)}(\tau) - B^{(1)}(\tau)] Q_j, \quad (\text{A33})$$

$$\delta T^i_j = 0. \quad (\text{A34})$$

For vector perturbations, Bardeen (1980) defined the gauge-invariant combinations:

$$\Psi = B^{(1)} - \frac{1}{q} H_T^{(1)'}, \quad (\text{A35})$$

$$V_c = V^{(1)} - B^{(1)}. \quad (\text{A36})$$

The perturbation equation (A1) for these vector gauge-invariant variables are given by Bardeen (1980):

$$(q^2 - 2K)\Psi = 16\pi G a^2 \bar{\rho} V_c, \quad (\text{A37})$$

$$V_c' + \frac{a'}{a} V_c = 0. \quad (\text{A38})$$

We define a new variable $v_T = a^{-1} V_c$, which is the transverse part of the velocity v^i . After superposing the modes of the equation (A38), we obtain

$$\dot{v}_T^i + 2H v_T^i = 0, \quad (\text{A39})$$

$$\nabla_i v_T^i = 0. \quad (\text{A40})$$

Since the density contrast and the velocity field are irrelevant to the tensor perturbations, we do not repeat here equations of motion for tensor perturbations. Complete equations to determine the density contrast and the velocity field is given by equations (A22)–(A24) and (A39), where velocity field is decomposed into the longitudinal part and the transverse part, as $v^i = \nabla^i \psi + v_T^i$. The equation (A39) is immediately integrated to give

$$v_T^i \propto a^{-2}, \quad (\text{A41})$$

i.e., the transverse part decays with time. This result is the consequence of the fact that the matter is pressureless. In summary, neglecting the decaying transverse mode, the complete equations to determine the density contrast and the velocity field is given by equations (A22)–(2.21), where the velocity consists of purely longitudinal part.

APPENDIX B ORTHONORMAL SET OF LAPLACIAN IN THREE DIMENSIONAL SPACES WITH CONSTANT CURVATURES

In this appendix, we construct the orthonormal set of the Laplacian in a space with or without spatial curvature and derive the expression of the correlation function in real space in terms of the power spectrum, when the spatial curvature is not negligible.

B.1. Harmonic Functions

The Laplacian of a function Q in the metric γ_{ij} of the equations (2.3) and (2.1) is given by

$$\Delta Q = \begin{cases} \frac{-K}{\sinh^2 \chi} \left[\frac{\partial}{\partial \chi} \left(\sinh^2 \chi \frac{\partial Q}{\partial \chi} \right) + \frac{1}{\sin \theta} \frac{\partial}{\partial \theta} \left(\sin \theta \frac{\partial Q}{\partial \theta} \right) + \frac{1}{\sin^2 \theta} \frac{\partial^2 Q}{\partial \phi^2} \right], & (K < 0) \\ \frac{1}{\chi^2} \left[\frac{\partial}{\partial \chi} \left(\chi^2 \frac{\partial Q}{\partial \chi} \right) + \frac{1}{\sin \theta} \frac{\partial}{\partial \theta} \left(\sin \theta \frac{\partial Q}{\partial \theta} \right) + \frac{1}{\sin^2 \theta} \frac{\partial^2 Q}{\partial \phi^2} \right], & (K = 0) \\ \frac{K}{\sin^2 \chi} \left[\frac{\partial}{\partial \chi} \left(\sin^2 \chi \frac{\partial Q}{\partial \chi} \right) + \frac{1}{\sin \theta} \frac{\partial}{\partial \theta} \left(\sin \theta \frac{\partial Q}{\partial \theta} \right) + \frac{1}{\sin^2 \theta} \frac{\partial^2 Q}{\partial \phi^2} \right], & (K > 0) \end{cases} \quad (\text{B1})$$

To evaluate the inverse Laplacian, it is useful to obtain a complete set of scalar harmonic functions satisfying the Helmholtz equation (Harrison 1967; Wilson 1983)

$$(\Delta + q^2)Q = 0. \quad (\text{B2})$$

If we separate variables, the angular part of the solution is just a spherical harmonic $Y_l^m(\theta, \phi)$. The radial part $X_l(\chi)$, associated with Y_l^m satisfies the following radial equation,

$$\frac{1}{\sinh^2 \chi} \frac{\partial}{\partial \chi} \left(\sinh^2 \chi \frac{\partial X_l}{\partial \chi} \right) + \left[\nu^2 + 1 - \frac{l(l+1)}{\sinh^2 \chi} \right] X_l = 0, \quad (K < 0) \quad (\text{B3})$$

$$\frac{1}{\chi^2} \frac{\partial}{\partial \chi} \left(\chi^2 \frac{\partial X_l}{\partial \chi} \right) + \left[\nu^2 - \frac{l(l+1)}{\chi^2} \right] X_l = 0, \quad (K = 0) \quad (\text{B4})$$

$$\frac{1}{\sin^2 \chi} \frac{\partial}{\partial \chi} \left(\sin^2 \chi \frac{\partial X_l}{\partial \chi} \right) + \left[\nu^2 - 1 - \frac{l(l+1)}{\sin^2 \chi} \right] X_l = 0, \quad (K > 0) \quad (\text{B5})$$

where we introduce a new variable ν as follows

$$q^2 = -K(\nu^2 + 1), \quad (K < 0) \quad (\text{B6})$$

$$q^2 = \nu^2, \quad (K = 0) \quad (\text{B7})$$

$$q^2 = K(\nu^2 - 1). \quad (K > 0) \quad (\text{B8})$$

The solutions of radial equations (B3)–(B5) which are regular at the origin are given by conical functions, Bessel functions, and toroidal functions for negative, zero, and positive curvature, respectively (e.g., Harrison 1967; Abbott & Schaefer 1986):

$$\begin{aligned} X_l^{(-)}(\nu, \chi) &= (-1)^l M_l^{(-)}(\nu) \sqrt{\frac{\pi}{2 \sinh \chi}} \mathcal{P}_{-1/2+i\nu}^{-1/2-l}(\cosh \chi) \\ &= \frac{\sinh^l \chi}{\nu} \frac{d^l}{d(\cosh \chi)^l} \left(\frac{\sin \nu \chi}{\sinh \chi} \right), \quad \nu^2 \geq 0, \quad (K < 0) \end{aligned} \quad (\text{B9})$$

$$X_l^{(0)}(\nu, \chi) = (-1)^l \nu^l j_l(\nu\chi) = \frac{\chi^l}{\nu} \left(\frac{1}{\chi} \frac{\partial}{\partial \chi} \right)^l \left(\frac{\sin \nu\chi}{\chi} \right), \quad \nu^2 \geq 0, \quad (K = 0) \quad (\text{B10})$$

$$\begin{aligned} X_l^{(+)}(\nu, \chi) &= (-1)^l M_l^{(+)}(\nu) \sqrt{\frac{\pi}{2 \sin \chi}} P_{-1/2+\nu}^{-1/2-l}(\cos \chi) \\ &= \frac{(-1)^l \sin^l \chi}{\nu} \frac{d^l}{d(\cos \chi)^l} \left(\frac{\sin \nu\chi}{\sin \chi} \right), \quad \nu = 2, 3, 4, \dots, \quad (K > 0) \quad (\text{B11}) \end{aligned}$$

where \mathcal{P}_ν^μ is the associated Legendre function, and $P_\nu^\mu(x) = e^{i\pi\mu/2} \mathcal{P}_\nu^\mu(x+i0)$ is the associated Legendre function on the cut (Magnus, Oberhettinger & Soni 1966). The spectrum for the space of positive curvature is discrete because of the condition that the function is periodic, or single-valued. We introduce notations, $M_l^{(\mp)}(\nu) = (\nu^2 \pm 1^2)(\nu^2 \pm 2^2) \cdots (\nu^2 \pm l^2)$, and $M_0^{(\pm)} \equiv 1$. We can see that $X_l^{(+)}(\nu, \chi) = i^l X_l^{(-)}(-i\nu, i\chi)$ by analytic continuation with a natural choice of branches. For $\chi \rightarrow 0$, all these functions behave like χ^l with appropriate constants, and thus $X_l(\nu, 0) = \delta_{l0}$ (e.g., Harrison 1967). For the variable ν is positive integers in closed universe, $X_l^{(+)}$ can also be represented by Gegenbauer (or ultraspherical) polynomials $C_n^\lambda(x)$ as

$$X_l^{(+)}(\nu, \chi) = \frac{(-2)^l l! \sin^l \chi}{\nu} C_{\nu-l-1}^{l+1}(\cos \chi). \quad (\text{B12})$$

We choose normalizations so that $K \rightarrow 0$ limit of either equation (B9) or (B11) reduces to equation (B10). In these normalizations, the derivatives and recursion relations for X_l are particularly simple. In fact, the derivatives of the radial functions are simply given by

$$\frac{\partial}{\partial \chi} \left(\frac{X_l^{(-)}(\nu, \chi)}{\sinh^l \chi} \right) = \frac{X_{l+1}^{(-)}(\nu, \chi)}{\sinh^l \chi}, \quad (K < 0) \quad (\text{B13})$$

$$\frac{\partial}{\partial \chi} \left(\frac{X_l^{(0)}(\nu, \chi)}{\chi^l} \right) = \frac{X_{l+1}^{(0)}(\nu, \chi)}{\chi^l}, \quad (K = 0) \quad (\text{B14})$$

$$\frac{\partial}{\partial \chi} \left(\frac{X_l^{(+)}(\nu, \chi)}{\sin^l \chi} \right) = \frac{X_{l+1}^{(+)}(\nu, \chi)}{\sin^l \chi}, \quad (K > 0) \quad (\text{B15})$$

and the recursion relations, which are derived by the fact that X_l are the solution of the radial equations (B3)–(B5), are

$$(\nu^2 + l^2) X_{l-1}^{(-)}(\nu, \chi) + (2l+1) \frac{\cosh \chi}{\sinh \chi} X_l^{(-)}(\nu, \chi) + X_{l+1}^{(-)}(\nu, \chi) = 0, \quad (K < 0) \quad (\text{B16})$$

$$\nu^2 X_{l-1}^{(0)}(\nu, \chi) + \frac{2l+1}{\chi} X_l^{(0)}(\nu, \chi) + X_{l+1}^{(0)}(\nu, \chi) = 0, \quad (K = 0) \quad (\text{B17})$$

$$(\nu^2 - l^2) X_{l-1}^{(+)}(\nu, \chi) + (2l+1) \frac{\cos \chi}{\sin \chi} X_l^{(+)}(\nu, \chi) + X_{l+1}^{(+)}(\nu, \chi) = 0. \quad (K > 0) \quad (\text{B18})$$

In this paper, we need only $l = 0, 1, 2, 3, 4$ for the evaluation of redshift distortion. They are given by

$$X_0^{(-)} = \frac{\sin \nu \chi}{\nu \sinh \chi}, \quad (\text{B19})$$

$$X_1^{(-)} = \frac{1}{\nu \sinh^2 \chi} (-\cosh \chi \sin \nu \chi + \nu \sinh \chi \cos \nu \chi), \quad (\text{B20})$$

$$X_2^{(-)} = \frac{1}{\nu \sinh^3 \chi} \left\{ [3 - (\nu^2 - 2) \sinh^2 \chi] \sin \nu \chi - 3\nu \sinh \chi \cosh \chi \cos \nu \chi \right\}, \quad (\text{B21})$$

$$X_3^{(-)} = \frac{1}{\nu \sinh^4 \chi} \left\{ \cosh \chi [-15 + 6(\nu^2 - 1) \sinh^2 \chi] \sin \nu \chi \right. \\ \left. + \nu \sinh \chi [15 - (\nu^2 - 11) \sinh^2 \chi] \cos \nu \chi \right\}, \quad (\text{B22})$$

$$X_4^{(-)} = \frac{1}{\nu \sinh^5 \chi} \left\{ [105 - 15(3\nu^2 - 8) \sinh^2 \chi + (\nu^4 - 35\nu^2 + 24) \sinh^4 \chi] \sin \nu \chi \right. \\ \left. - \nu \sinh \chi [105 - 10(\nu^2 - 5) \sinh^2 \chi] \cos \nu \chi \right\}, \quad (\text{B23})$$

for $K < 0$, and

$$X_0^{(0)} = \frac{\sin \nu \chi}{\nu \chi}, \quad (\text{B24})$$

$$X_1^{(0)} = \frac{1}{\nu \chi^2} (-\sin \nu \chi + \nu \chi \cos \nu \chi), \quad (\text{B25})$$

$$X_2^{(0)} = \frac{1}{\nu \chi^3} \left[(3 - \nu^2 \chi^2) \sin \nu \chi - 3\nu \chi \cos \nu \chi \right], \quad (\text{B26})$$

$$X_3^{(0)} = \frac{1}{\nu \chi^4} \left[(-15 + 6\nu^2 \chi^2) \sin \nu \chi + \nu \chi (15 - \nu^2 \chi^2) \cos \nu \chi \right], \quad (\text{B27})$$

$$X_4^{(0)} = \frac{1}{\nu \chi^5} \left[(105 - 45\nu^2 \chi^2 + \nu^4 \chi^4) \sin \nu \chi - \nu \chi (105 - 10\nu^2 \chi^2) \cos \nu \chi \right], \quad (\text{B28})$$

for $K = 0$, and

$$X_0^{(+)} = \frac{\sin \nu \chi}{\nu \sin \chi}, \quad (\text{B29})$$

$$X_1^{(+)} = \frac{1}{\nu \sin^2 \chi} (-\cos \chi \sin \nu \chi + \nu \sin \chi \cos \nu \chi), \quad (\text{B30})$$

$$X_2^{(+)} = \frac{1}{\nu \sin^3 \chi} \left\{ [3 - (\nu^2 + 2) \sin^2 \chi] \sin \nu \chi - 3\nu \sin \chi \cos \chi \cos \nu \chi \right\}, \quad (\text{B31})$$

$$X_3^{(+)} = \frac{1}{\nu \sin^4 \chi} \left\{ \cosh \chi [-15 + 6(\nu^2 + 1) \sin^2 \chi] \sin \nu \chi \right. \\ \left. + \nu \sin \chi [15 - (\nu^2 + 11) \sin^2 \chi] \cos \nu \chi \right\}, \quad (\text{B32})$$

$$X_4^{(+)} = \frac{1}{\nu \sin^5 \chi} \left\{ [105 - 15(3\nu^2 + 8) \sin^2 \chi + (\nu^4 + 35\nu^2 + 24) \sin^4 \chi] \sin \nu \chi \right.$$

$$- \nu \sin \chi \left[105 - 10(\nu^2 + 5) \sin^2 \chi \right] \cos \nu \chi \Big\}, \quad (\text{B33})$$

for $K > 0$.

Although our normalizations in equations (B9)–(B11) have simple relations for derivatives and recursion relations, it is also convenient to introduce further normalizations as

$$\widehat{X}_l^{(\mp)}(\nu, \chi) = \frac{X_l^{(\mp)}(\nu, \chi)}{\sqrt{M^{(\mp)}(\nu)}}, \quad \widehat{X}_l^{(0)}(\nu, \chi) = \frac{X_l^{(0)}(\nu, \chi)}{\nu^l} = (-1)^l j_l(\nu \chi) \quad (\text{B34})$$

From the orthogonality and completeness of conical functions, Bessel functions, and Gegenbauer polynomials (Magnus et al. 1966), we can find

$$4\pi \int \sinh^2 \chi d\chi \widehat{X}_l^{(-)}(\nu, \chi) \widehat{X}_l^{(-)}(\nu', \chi) = \frac{2\pi^2}{\nu^2} \delta(\nu - \nu'), \quad (K < 0) \quad (\text{B35})$$

$$4\pi \int \chi^2 d\chi \widehat{X}_l^{(0)}(\nu, \chi) \widehat{X}_l^{(0)}(\nu', \chi) = \frac{2\pi^2}{\nu^2} \delta(\nu - \nu'), \quad (K = 0) \quad (\text{B36})$$

$$4\pi \int \sin^2 \chi d\chi \widehat{X}_l^{(+)}(\nu, \chi) \widehat{X}_l^{(+)}(\nu', \chi) = \frac{2\pi^2}{\nu^2} \delta_{\nu\nu'}, \quad (K > 0) \quad (\text{B37})$$

and

$$\int \frac{\nu^2 d\nu}{2\pi^2} \widehat{X}_l^{(-)}(\nu, \chi) \widehat{X}_l^{(-)}(\nu, \chi') = \frac{\delta(\chi - \chi')}{4\pi \sinh^2 \chi}, \quad (K < 0) \quad (\text{B38})$$

$$\int \frac{\nu^2 d\nu}{2\pi^2} \widehat{X}_l^{(0)}(\nu, \chi) \widehat{X}_l^{(0)}(\nu, \chi') = \frac{\delta(\chi - \chi')}{4\pi \chi^2}, \quad (K = 0) \quad (\text{B39})$$

$$\sum_{\nu=2}^{\infty} \frac{\nu^2}{2\pi^2} \widehat{X}_l^{(+)}(\nu, \chi) \widehat{X}_l^{(+)}(\nu, \chi') = \frac{\delta(\chi - \chi')}{4\pi \sin^2 \chi}. \quad (K > 0) \quad (\text{B40})$$

B.2. The Correlation Function in Real Space at Present Time

The density contrast $\delta(\chi, \theta, \phi)$ is expanded in terms of the eigenfunctions as follows:

$$\delta(\chi, \theta, \phi) = \sum_{l=0}^{\infty} \sum_{m=-l}^l \int \frac{\nu^2 d\nu}{2\pi^2} \tilde{\delta}_{lm}(\nu) \widehat{X}_l^{(-)}(\nu, \chi) Y_l^m(\theta, \phi), \quad (K < 0) \quad (\text{B41})$$

$$\delta(\chi, \theta, \phi) = \sum_{l=0}^{\infty} \sum_{m=-l}^l \int \frac{\nu^2 d\nu}{2\pi^2} \tilde{\delta}_{lm}(\nu) \widehat{X}_l^{(0)}(\nu, \chi) Y_l^m(\theta, \phi), \quad (K = 0) \quad (\text{B42})$$

$$\delta(\chi, \theta, \phi) = \sum_{l=0}^{\infty} \sum_{m=-l}^l \sum_{\nu=3}^{\infty} \frac{\nu^2}{2\pi^2} \tilde{\delta}_{lm}(\nu) \widehat{X}_l^{(+)}(\nu, \chi) Y_l^m(\theta, \phi). \quad (K > 0) \quad (\text{B43})$$

For a positive curvature model, the term of $\nu = 2$ is omitted because $\nu = 2$ corresponds to a mode which is a pure gauge term (Lifshitz & Khalatnikov 1963; Bardeen 1980) as indicated by equation (A18). The inverse of these expansion is

$$\tilde{\delta}_{lm}(\nu) = 4\pi \int \sinh^2 \chi d\chi \int \sin \theta d\theta d\phi \delta(\chi, \theta, \phi) \widehat{X}_l^{(-)}(\nu, \chi) Y_l^{m*}(\theta, \phi), \quad (K < 0) \quad (\text{B44})$$

$$\tilde{\delta}_{lm}(\nu) = 4\pi \int \chi^2 d\chi \int \sin \theta d\theta d\phi \delta(\chi, \theta, \phi) \widehat{X}_l^{(0)}(\nu, \chi) Y_l^{m*}(\theta, \phi), \quad (K = 0) \quad (\text{B45})$$

$$\tilde{\delta}_{lm}(\nu) = 4\pi \int \sin^2 \chi d\chi \int \sin \theta d\theta d\phi \delta(\chi, \theta, \phi) \widehat{X}_l^{(+)}(\nu, \chi) Y_l^{m*}(\theta, \phi). \quad (K > 0) \quad (\text{B46})$$

Since the correlation function $\xi(\chi)$ depends only on the separation of two points, and does not depend on the particular choice of the coordinate system, we can write it down as

$$\begin{aligned} \xi(\chi) &= \langle \delta(0, \theta, \phi) \delta(\chi, \theta, \phi) \rangle \\ &= \sum_{l,m} \sum_{l',m'} \int \frac{\nu^2 d\nu}{2\pi^2} \int \frac{\nu'^2 d\nu'}{2\pi^2} \\ &\quad \times \widehat{X}_l^{(-,0)}(\nu, 0) \widehat{X}_{l'}^{(-,0)}(\nu', \chi) Y_l^{m*}(\theta, \phi) Y_{l'}^{m'}(\theta, \phi) \langle \tilde{\delta}_{lm}^*(\nu) \tilde{\delta}_{l'm'}(\nu') \rangle, \quad (K \leq 0) \quad (\text{B47}) \end{aligned}$$

$$\begin{aligned} \xi(\chi) &= \langle \delta(0, \theta, \phi) \delta(\chi, \theta, \phi) \rangle \\ &= \sum_{l,m} \sum_{l',m'} \sum_{\nu=3}^{\infty} \frac{\nu^2}{2\pi^2} \sum_{\nu'=3}^{\infty} \frac{\nu'^2}{2\pi^2} \\ &\quad \times \widehat{X}_l^{(+)}(\nu, 0) \widehat{X}_{l'}^{(+)}(\nu', \chi) Y_l^{m*}(\theta, \phi) Y_{l'}^{m'}(\theta, \phi) \langle \tilde{\delta}_{lm}^*(\nu) \tilde{\delta}_{l'm'}(\nu') \rangle. \quad (K > 0) \quad (\text{B48}) \end{aligned}$$

Statistical homogeneity and isotropy of the universe suggest that correlation of modes has the form

$$\langle \tilde{\delta}_{lm}^*(\nu) \tilde{\delta}_{l'm'}(\nu') \rangle = (2\pi)^3 \delta_{ll'} \delta_{mm'} \frac{\delta(\nu - \nu')}{\nu^2} S(\nu), \quad (K \leq 0) \quad (\text{B49})$$

$$\langle \tilde{\delta}_{lm}^*(\nu) \tilde{\delta}_{l'm'}(\nu') \rangle = (2\pi)^3 \delta_{ll'} \delta_{mm'} \frac{\delta_{\nu\nu'}}{\nu^2} S(\nu), \quad (K > 0) \quad (\text{B50})$$

where $S(\nu)$ is a power spectrum of the number density field at present. From this equation and $X_l(\nu, 0) = \delta_{l0}$, equations (B47) and (B48) reduce to

$$\xi(\chi) = \int \frac{\nu^2 d\nu}{2\pi^2} X_0^{(-,0)}(\nu, \chi) S(\nu), \quad (K \leq 0) \quad (\text{B51})$$

$$\xi(\chi) = \sum_{\nu=3}^{\infty} \frac{\nu^2}{2\pi^2} X_0^{(+)}(\nu, \chi) S(\nu). \quad (K > 0) \quad (\text{B52})$$

The equation (B51) is an equivalent formula that Wilson (1983) has previously derived. These formulas can be even transformed to the forms more like the usual formula:

$$\xi(x) = \int \frac{k^2 dk}{2\pi^2} P(k) \frac{\sqrt{-K} \sin(kx)}{k \sinh(\sqrt{-K}x)}, \quad (K < 0) \quad (\text{B53})$$

$$\xi(x) = \int \frac{k^2 dk}{2\pi^2} P(k) \frac{\sin(kx)}{kx}, \quad (K = 0) \quad (\text{B54})$$

$$\xi(x) = \sum_{i=1}^{\infty} \frac{k_i^2 \sqrt{K}}{2\pi^2} P(k_i) \frac{\sqrt{K} \sin(k_i x)}{k_i \sin(\sqrt{K} x)}, \quad (K > 0) \quad (\text{B55})$$

where the discrete wave number, $k_i = (i+2)\sqrt{K}$, is for the space of positive curvature. The relations between usual power spectrum $P(k)$ and the power spectrum $S(\nu)$ are given by

$$P(k) = \frac{S(|K|^{-1/2}k)}{|K|^{3/2}}, \quad (K \neq 0) \quad (\text{B56})$$

$$P(k) = S(k), \quad (K = 0) \quad (\text{B57})$$

When the scale of interest is much smaller than the curvature scale, $x \ll |K|^{-1/2}$, both expressions (B53) for negative curvature and (B55) for positive curvature reduce to the familiar expression (B54).

Finally, we comment that comparing the expression $\xi(\chi) = \langle \delta(\chi_1, \theta_1, \phi_1) \delta(\chi_2, \theta_2, \phi_2) \rangle$ and the expression (B51) or (B52) proves the addition theorem for $\widehat{X}_l = \widehat{X}_l^{(\pm,0)}$:

$$\widehat{X}_0(\nu, \chi) = \sum_l (2l+1) \widehat{X}_l(\nu, \chi_1) \widehat{X}_l(\nu, \chi_2) P_l(\cos \theta). \quad (\text{B58})$$

For the flat case $K = 0$, the above equation is nothing but the well-known addition theorem of the Bessel function, therefore, the addition theorem for $K \neq 0$ is the generalizations of it to the constant curvature space.

REFERENCES

- Abbott, L. F. & Schaefer, R. K. 1986, *ApJ*, 308, 546
- Alcock, C. & Paczyński, B. 1979, *Nature*, 281, 358
- Ballinger, W. E. & Peacock, J. A. & Heavens, A. F. 1996, *MNRAS*, 276, L59
- Bardeen, J. M. 1980, *Phys.Rev.*, D22, 1882
- Bardeen, J. M., Bond, J. R., Kaiser, N. & Szalay, A. S. 1986, *ApJ*, 304, 15
- Bernardeau, F., van Waerbeke, L. & Mellier, Y. 1997, *A&A*, 322, 1
- Bharadwaj, S. 1999, *ApJ*, 516, 507
- Colless, M. 1998, *Phil.Trans.R.Soc.Lond.*, to appear (astro-ph/9804079)
- de Laix, A. A. & Starkman, G. 1998, *ApJ*, 501, 427
- Fisher, K. B., Scharf, C. & Lahav O. 1994, *MNRAS*, 266, 219
- Folkes, S. R. et al. 1999, *MNRAS*, 308, 459
- Hamilton, A. J. S. 1992, *ApJ*, 385, L5
- Hamilton, A. J. S. 1998, in *The Evolving Universe: Selected Topics on Large-Scale Structure and on the Properties of Galaxies*, ed. Hamilton, D. (Dordrecht: Kluwer Academic Publishers), p.185, (astro-ph/9708102)
- Hamilton, A. J. S. & Culhane, M. 1996, *MNRAS*, 278, 73
- Harrison, E. R. 1967, *Rev. Mod. Phys.*, 39, 862
- Heavens, A. F. & Taylor, A. N. 1995, *MNRAS*, 275, 483
- Hwang, J.-C. & Vishniac, E. T. 1990, *ApJ*, 353, 1
- Kaiser, N. 1987, *MNRAS*, 227, 1
- Kaiser, N. 1992, *ApJ*, 388, 272
- Kaiser, N. 1998, *ApJ*, 498, 26
- Kodama, H. & Sasaki, M. 1984, *Prog. Theor. Phys. Suppl.*, 78, 1
- Kogut, A., et al. 1993, *ApJ*, 419, 1

- Lahav, O., Lilje, P. B., Primack, J. R. & Rees, M. J. 1991, MNRAS, 251, 128
- Lifshitz, E. & Khalatnikov, I. 1963, Adv. Phys., 12, 185
- Lilje, P. B. & Efstathiou, G. 1989, MNRAS, 236, 851
- Lineweaver, C. H., Tenorio, L., Smoot, G. F., Keegstra, P., Banday, A. J. and Lubin, P. 1996, ApJ, 470, 38
- Lyth, D. H. & Stewart 1990, Phys. Lett., B252, 336
- McGill, C. 1990, MNRAS, 242, 428
- Magnus, W., Oberhettinger, F. & Soni, R. P. 1966, Formulas and Theorems for the Special Functions of Mathematical Physics (New York: Springer-Verlag)
- Margon, B. 1998, Phil.Trans.R.Soc.Lond. A, to appear (astro-ph/9805314)
- Matsubara, T. 1999, ApJ, 525, 543
- Matsubara, T. & Suto, Y. 1996, ApJ, 470, L1
- Matsubara, T., Szalay, A. S. & Landy, S. D. 1999, ApJ, submitted (astro-ph/9911151)
- Nair V. 1999, astro-ph/9904312
- Nakamura, T. T., Matsubara, T. & Suto, Y. 1998, ApJ, 494, 13
- Nishioka, H. & Yamamoto, K. 1999, ApJ, 520, 426
- Peebles, P. J. E. 1974, A&A, 32, 197
- Peebles, P. J. E. 1980, The Large-Scale Structure of the Universe (Princeton; Princeton University Press)
- Pen, U. 1998, ApJ, 504, 601
- Popowski, P. A., Weinberg, D. H., Ryden, B. S. & Osmer, P. S. 1998, ApJ, 498, 11
- Ratra, B. & Peebles, P. J. E. 1994, ApJ, 432, L5
- Sachs, R. W. & Wolfe, A. M. 1967, ApJ, 147, 73
- Strauss, M. A. 1999, in “Structure Formation in the Universe”, ed. Dekel and Ostriker, in press (astro-ph/9610033)

- Suto, Y., Magira, H., Jing, Y. P., Matsubara, T. & Yamamoto, K. 1999, *Prog. Theor. Phys. Suppl.*, 133, 183
- Szalay, A. S., Matsubara, T. & Landy, S. D. 1998, *ApJ*, 498, L1
- Totsuji, H. & Kihara, T. 1969, *PASJ*, 21, 221
- Vogeley, M. S. & Szalay, A. S. 1996, *ApJ*, 465, 34
- White, M. & Bunn, E. 1995, *ApJ*, 450, 477
- White, M. & Scott, D. 1996, *ApJ*, 459, 415
- Wilson, M. L. 1983, *ApJ*, 273, 2
- Zaroubi, S. & Hoffman, Y. 1996, *ApJ*, 462, 25

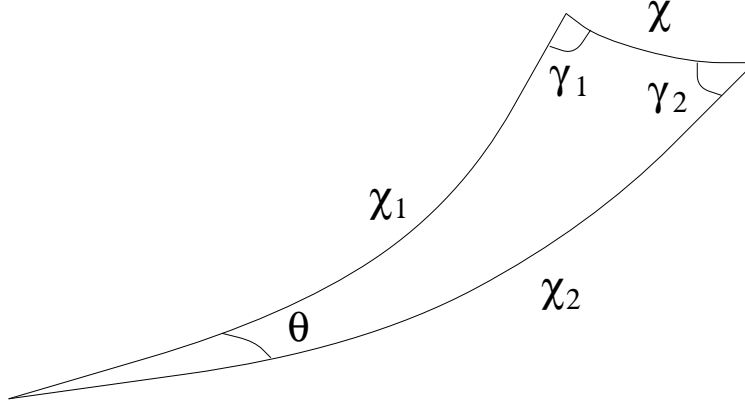


Fig. 1.— Geometry of the relative position of the observer and the two points. The space is not necessarily Euclidean.

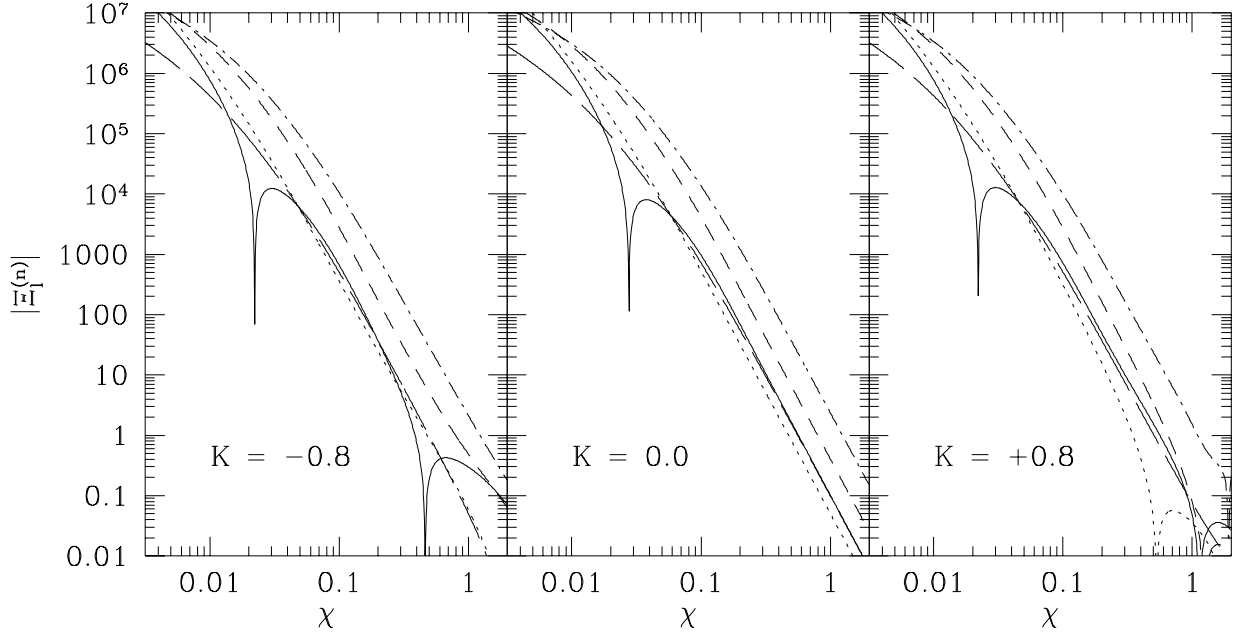


Fig. 2.— Some examples of the function $\Xi_i^{(n)}(\chi)$. The CDM-type power spectrum with $\Gamma = 0.2(h^{-1}\text{Mpc})^{-1}$ and “scale invariant” (see text) primordial spectrum is assumed and the normalization is arbitrary. The curvature is $K = -0.8, 0, +0.8$ from the left panel to the right panel. Solid lines: $\Xi_0^{(0)}$, dotted lines: $\Xi_0^{(1)}$, dashed lines: $\Xi_2^{(1)}$, long-dashed lines: $\Xi_2^{(2)}$, dash-dotted lines: $\Xi_4^{(2)}$.

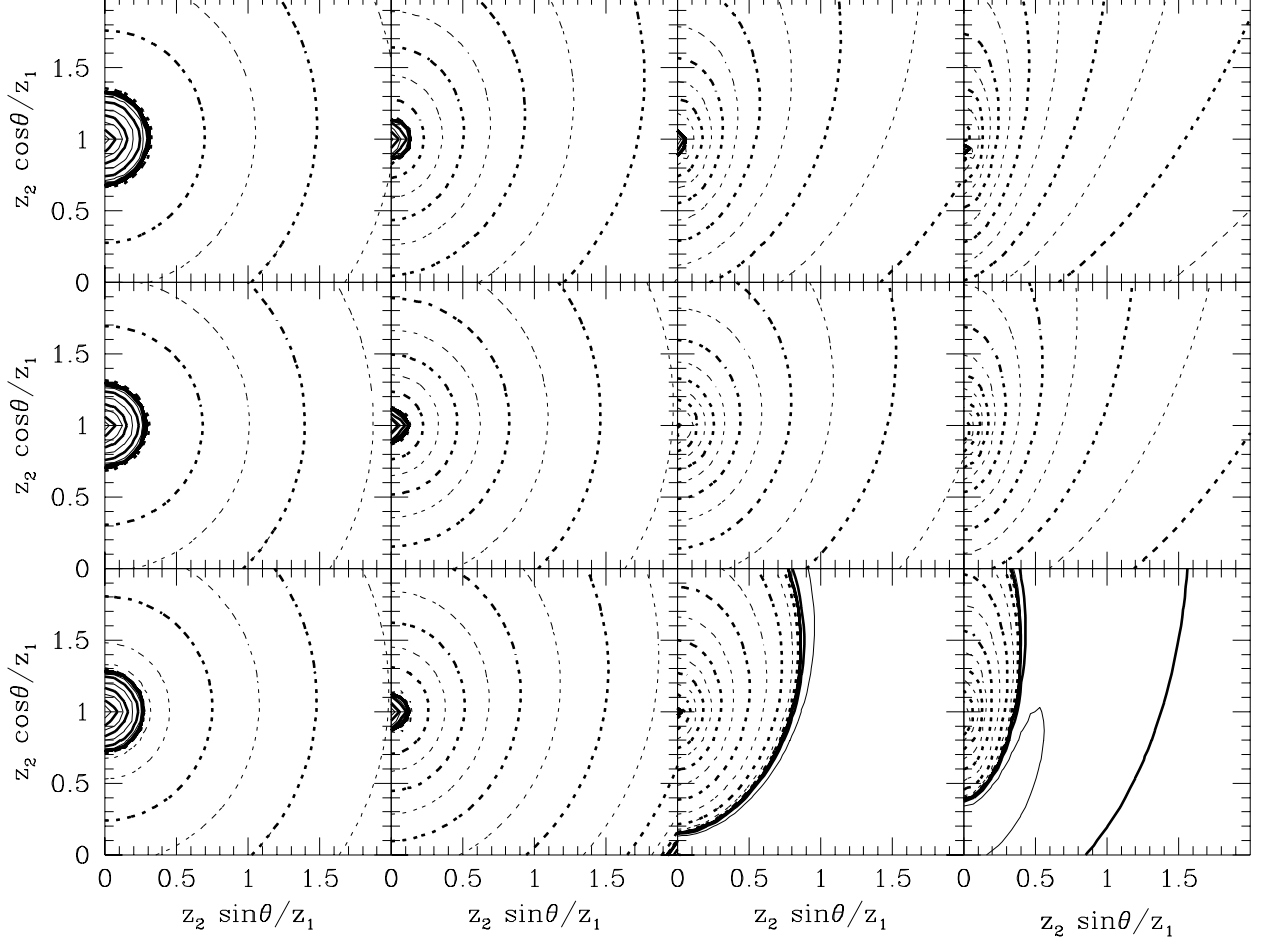


Fig. 3.— Contour plots of the correlation function in real space with purely geometrical distortions, without velocity distortions. The observer is sitting at the origin, and the first point at redshift z_1 is sitting at the center on the y-axis. The contour map shows the value of the correlation function depending on the position of the second point at redshift z_2 and angle θ . The solid lines indicate positive correlation and the dotted lines indicate the negative correlation. The normalization is arbitrary and the contour spacings are $\Delta \log_{10} |\xi| = 0.5$. The top panels are for the STD model ($\Omega_0 = 1$, $\lambda_0 = 0$), the middle for the FLAT model ($\Omega_0 = 0.2$, $\lambda_0 = 0.8$), and the bottom for the OPEN model ($\Omega_0 = 0.2$, $\lambda_0 = 0$). From left to right panels, the redshifts of the first point z_1 are 0.1, 0.3, 1, 3, respectively.

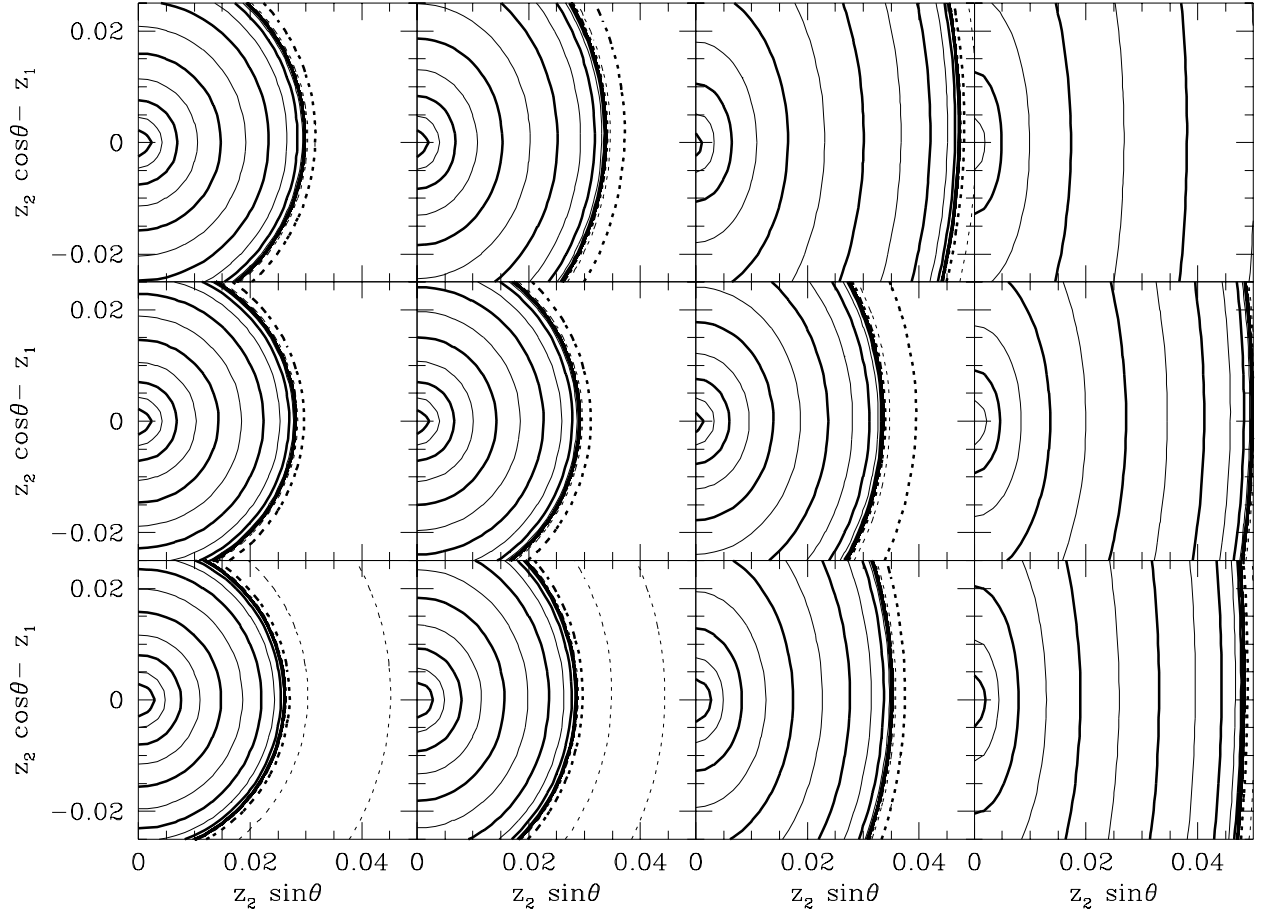


Fig. 4.— Same as Figure 3, but the scale of z around the first point is fixed. The observer is located at $(0, -z_1)$, which is outside of the plots.

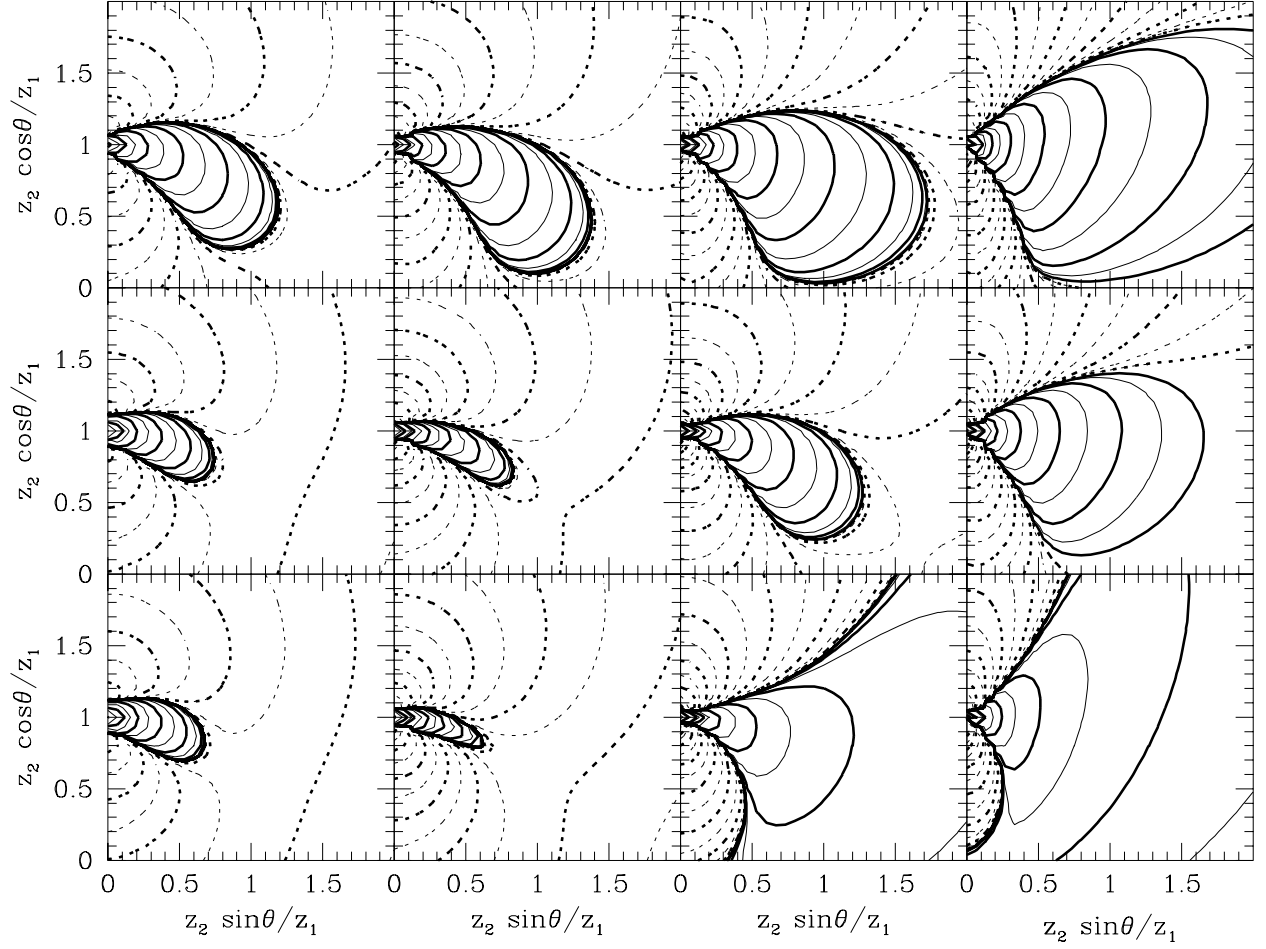


Fig. 5.— Contour plots of the correlation function in redshift space. The meaning of the panels are the same as in Figure 3, but the velocity distortions are included.

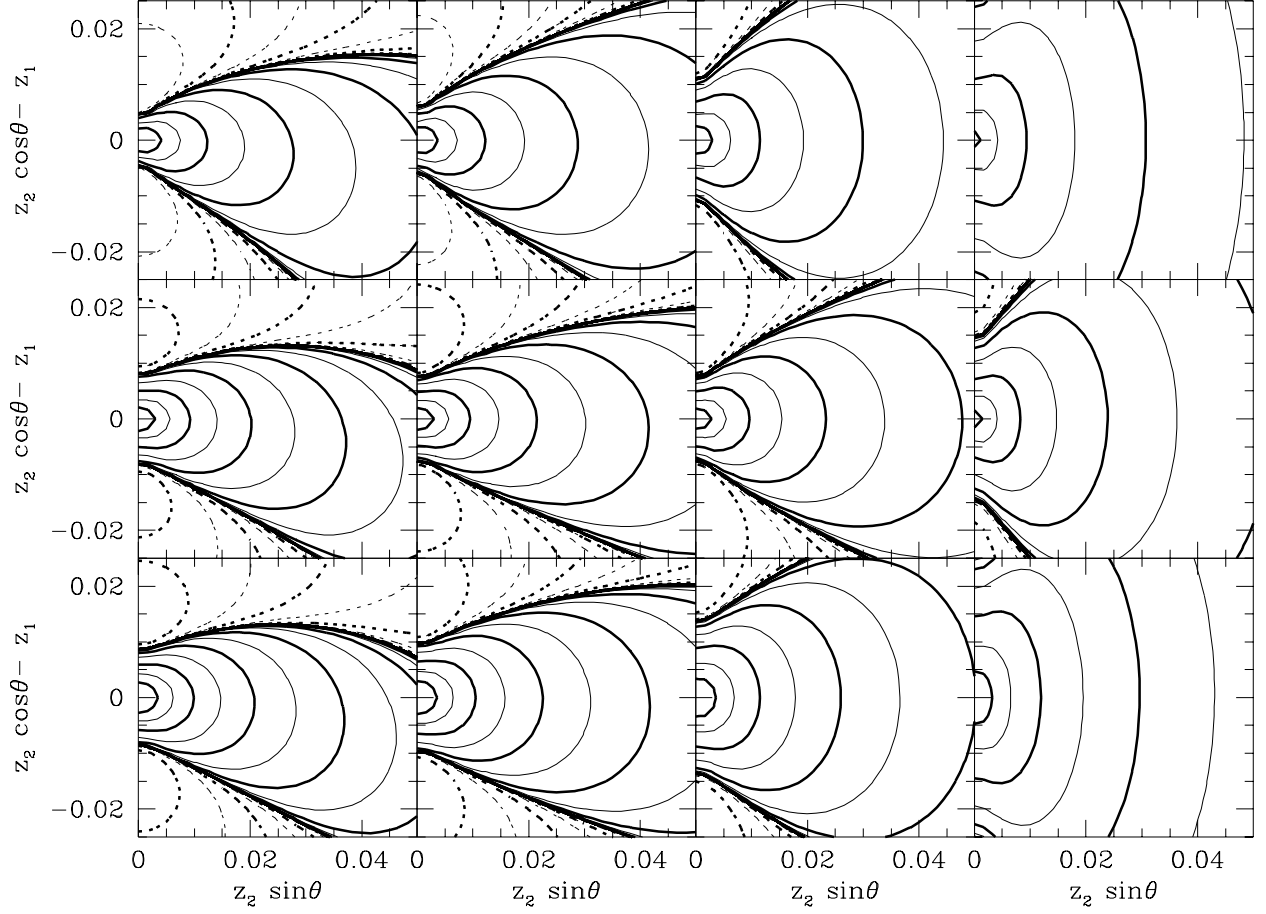


Fig. 6.— Contour plots of the correlation function in redshift space with fixed scale of z . The meaning of the panels are the same as in Figure 4, but the velocity distortions are included.

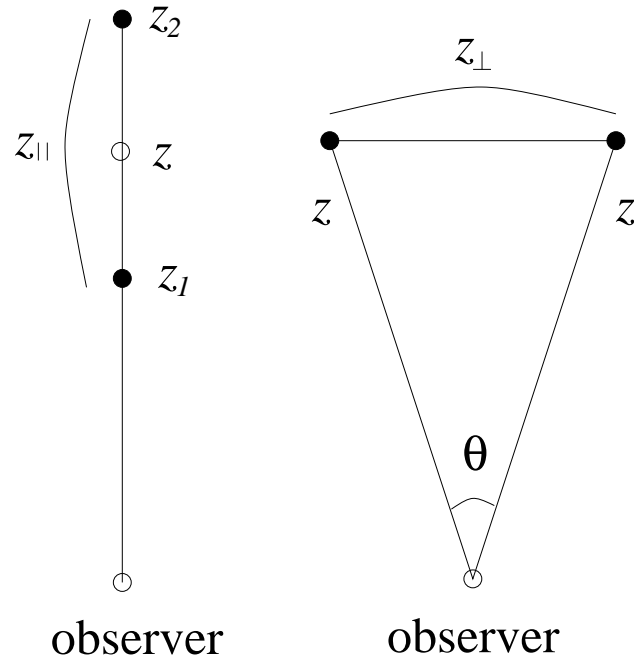


Fig. 7.— Geometrical meaning of the definition of the parallel redshift interval z_{\parallel} and the perpendicular redshift interval z_{\perp} .

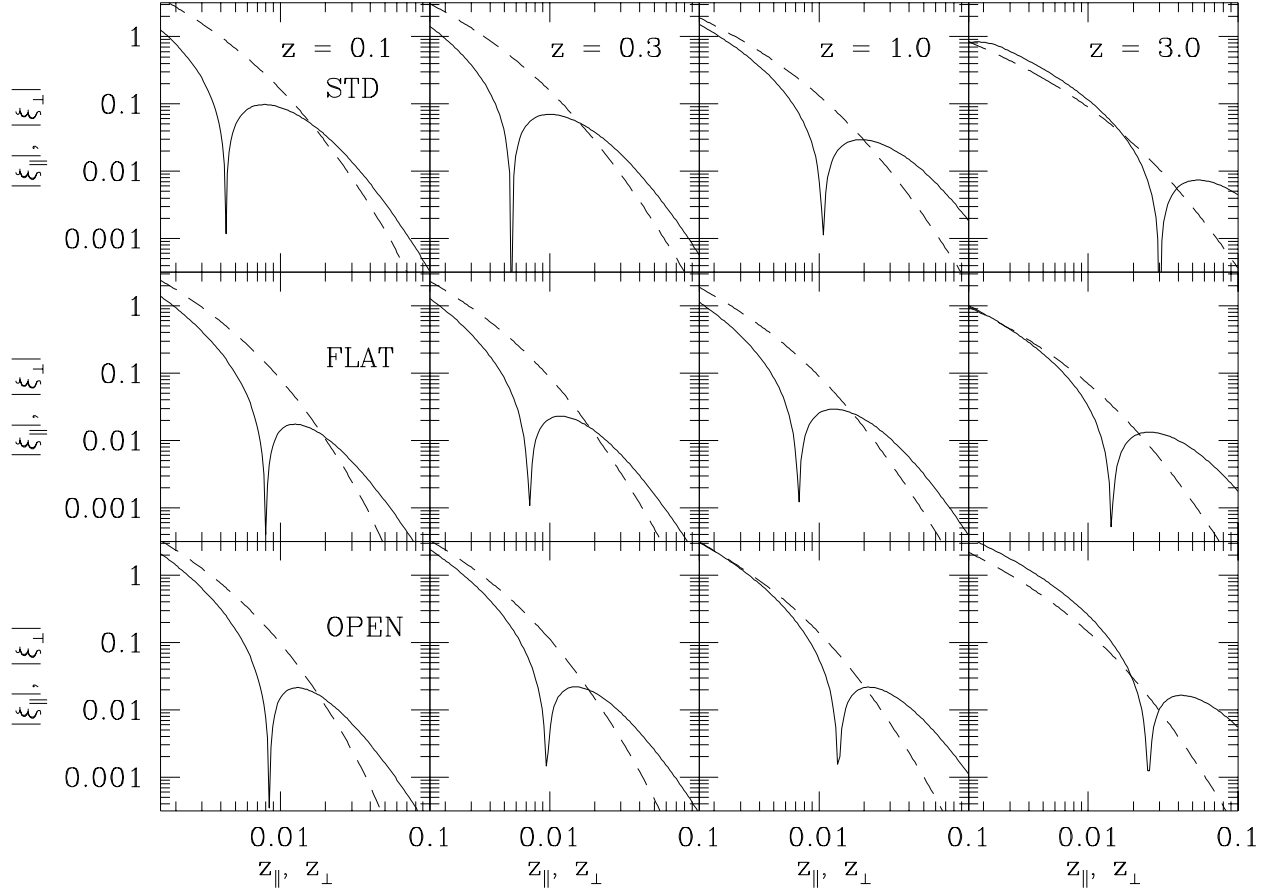


Fig. 8.— The parallel correlation function, ξ_{\parallel} (solid lines), and the perpendicular correlation function, ξ_{\perp} (dashed lines), in redshift space. The redshifts of the first point are 0.1, 0.3, 1, 3 from left to right panels. The cosmological models are STD, FLAT, and OPEN from top to bottom panels.

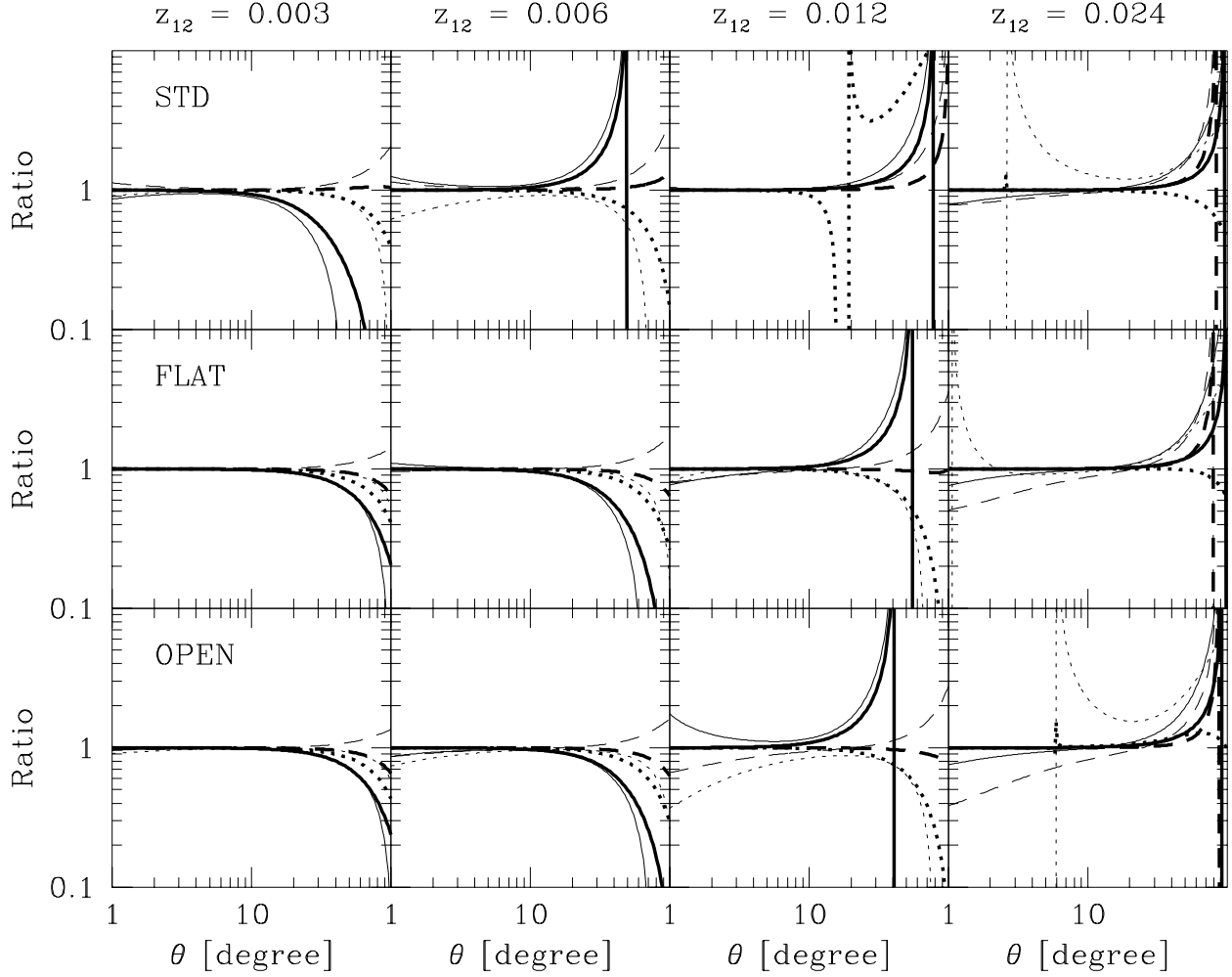


Fig. 9.— The ratio of the correlation functions by distant observer approximation to that of our result. The inclination angle γ_z (see text) is fixed to $\gamma_z = 10^\circ$ (solid lines), 45° (dotted lines), and 80° (dashed lines). The angle θ between the lines of sight is varied. The redshift separation z_{12} in velocity space is fixed to 0.003, 0.006, 0.012, 0.024 from left to right panels. Thin lines show the approximation by Hamilton (1992) for a nearby universe. Thick lines show the approximation by Matsubara & Suto (1996). Top, middle, bottom panels show each different cosmological models, STD, FLAT, and OPEN, respectively.